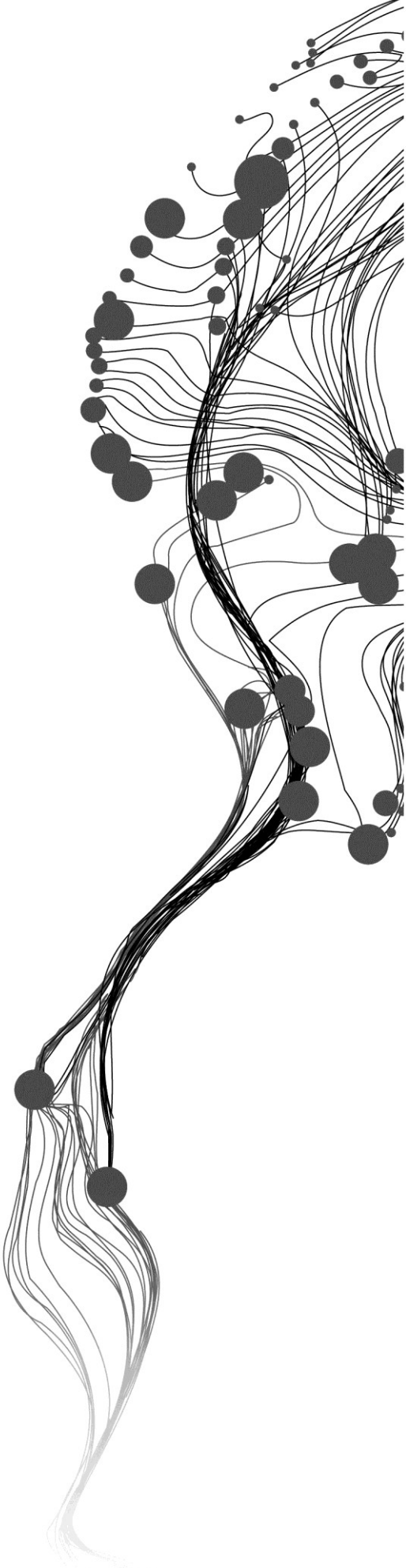


TEA BUSH BIOMASS ASSESSMENT THROUGH POLARIMETRIC DECOMPOSITION AND SEMI- EMPIRICAL MODELLING

ABHISHEK BANERJEE
March, 2012

SUPERVISORS:
Kumar, Shashi
Kushwaha, S.P.S.
Stein, Alfred
Bijker, Wietske



TEA BUSH BIOMASS ASSESSMENT THROUGH POLARIMETRIC DECOMPOSITION AND SEMI- EMPIRICAL MODELLING

ABHISHEK BANERJEE
Enschede, The Netherlands, March, 2012

Thesis submitted to the Faculty of Geo-Information Science and Earth Observation of the University of Twente in partial fulfilment of the requirements for the degree of Master of Science in Geo-information Science and Earth Observation.

Specialization: Geoinformatics

SUPERVISORS:
Kumar, Shashi
Kushwaha, S.P.S.
Stein, Alfred
Bijker, Wietske

THESIS ASSESSMENT BOARD:
Stein, Alfred (Chair)
Rao, Y.S. (External Examiner, IIT, Mumbai)
Kumar, Shashi (Supervisor)
Kushwaha, S.P.S. (Supervisor)
Bijker, W. (Supervisor)

DISCLAIMER

This document describes work undertaken as part of a programme of study at the Faculty of Geo-Information Science and Earth Observation of the University of Twente. All views and opinions expressed therein remain the sole responsibility of the author, and do not necessarily represent those of the Faculty.

ABSTRACT

Advances in remote sensing techniques lead the natural resource scientists, technologists and managers to apply in many important fronts like biomass estimation of vegetation (short and long height trees of forests), agricultural crops, and now of the important beverage the tea. The biomass of the forest has been an important parameter regarding global carbon stock modelling. The climate change and the global warming greatly influence the natural vegetation. The above ground biomass is also essential for carbon budget assessment and ecosystem productivity. The conventional remote sensing techniques are not yet capable of estimating the biomass much accurately, particularly, of low height vegetation with dense canopy structure such as tea-bushes. A continuous effort is being made at a faster pace to replace the traditional methods of biomass estimation with the polarimetric SAR technique. Especially, this is because of the SAR having higher penetration capability. Biomass estimation in the present scenario still remains a challenging task in inaccessible areas and low height vegetation. Bushes are quite different in structure as compared to the trees. They have low height and the canopy structure is often dense and thick. Optical imagery is often not capable of assessing the bushes and/or the bush parameters, which on the other hand is possible to some extent by the SAR data. Microwave backscatter is sensitive to vegetation features. Earlier attempts to estimate the biomass of the forests show appreciable results with SAR backscatter data. This prompted in the present study, to make an attempt to estimate the above ground biomass of the tea-bushes utilizing the concept of semi-empirical model together with the SAR data. Available literatures show that not much work has been done on the North-Eastern parts of India and, especially, on the biomass estimation of the tea-bushes; in spite of the fact that tea is one of the major beverages of the globe and India occupies the first position in the world, not only as the tea producer and consumer but also as the exporter of tea. The tea variety which India produces is one of its own kinds and has much demand all over the places in the world. However, tea-bush biomass estimation not only helps in identifying the growth and production of tea but also as carbon stock modelling. That is why, it appeals to work in the North-Eastern parts of India, the region of Assam, which has the largest and best tea estates in India.

The present study deals with the model based approach of the water cloud model to retrieve the above ground biomass of the tea-bushes. The model was integrated with the field measured data. The study area which covers the Sarusarai tea estate (Lat: 26.29° - 26.95° N and Long: 94.03° - 94.47° E) was visited for the collection of ground truth and tea inventory. The field survey revealed that there are lots of variations in the physical state of the tea-bushes due to the age and the year of plantations of tea. ALOS PALSAR data was used in the area under study. The SAR data was decomposed to retrieve the surface and volume scattering information. The model was trained with the help of the SAR data and the field measured data. The training provided the backscatter from ground, the two way transmissivity. The trained model was implemented to estimate the above ground biomass of the tea-bushes in the tea estates. The results show that the model gives better values for the biomass estimation. The validation of the model against ground measured data shows the capability of the model is good. The performance of the validated model is that it yielded the above ground tea-biomass with low root mean square error. The correlation was appreciably reasonable which assures the possibility and capability of the model for future routine use in the estimation of biomass of tea estates. Thus, the encouraging results out of the present study for tea-bushes indicate that there is definitely a high hope of estimating the above ground biomass and the bush parameters using the semi-empirical modelling approach utilizing polarimetric SAR data and *in-situ* measurements.

Keywords: SAR data, tea, tea-bushes, backscatter, above ground biomass, bush volume, polarimetry.

ACKNOWLEDGEMENTS

“God is Almighty”. I thank God (and not “Thank God!!!”) the most superior who makes me feel comfortable and energetic and fills some unknown sort of energy in me when I am exhausted or disappointed. He keeps me going.

I would thank my IIRS supervisors, Prof. S.P.S. Kushwaha and Mr. S. Kumar for their constant, inspirational and encouraging support and guidance. Their constant guidance resulted in bringing up this study and research work. Some people say “it is not only life which is important, but also how to lead and live it”. I learnt from them the details of research and how to find the motivations. I should always have a scientific approach and reasoning and should also try to think behind the scene. I should always make an attempt to find the reasons for the unquestioned work and frame questions related to the happening surrounding me. And thus find a suitable answer to it. This is what research means.

I want to thank my ITC supervisors, Prof. A. Stein and Dr. W. Bijker for their guidance and their support. The current work deals with tea bushes. It was Prof. Stein who made me interested on the tea bushes and motivated me to work on it. Thus I am grateful for the opportunity provided to me to work with all such eminent and talented supervisors both from IIRS and ITC. They have great potential, in depth knowledge, understanding and are filled with enthusiasm. It was a privilege for me working with them.

I wish to thank Dr. N. Hamm for his constant support both during my stay in Netherlands and also in India. He took good care regarding what all arrangements were needed; whatever and whenever required. He made the communication between my supervisors at ITC and me possible and was always careful for the arrangements, dates regarding reports, thesis, presentations, etc.

My general appreciation extends to all ITC staff and faculty members who made my stay at ITC graceful, pleasing and delightful.

My special thanks to Dr. Burman, (Tea Experimental Station, Toklai), whose support and positive approach assisted a lot in carrying out the field work. My sincere thanks and regards to the TRS/TES, Jorhat, Assam for the hospitality and the generous support extended to me which made my stay at Toklai pleasant, tension free and memorable. I also appreciate the help extended to me by the Toklai library.

They say “Parents are next to God”, I believe yes, they are indeed. Their moral support and guidance mean a lot to me. I also thank my mother from the bottom of my heart for her great moral support. They acted not only as my friends but also as my supervisor. I would take this opportunity to thank Prof. M. Banerjee, my father, who always supported me and helped me often in the crucial stages when I felt helpless during my work. His valuable suggestions and comments helped me improve my work and his in-depth suggestions kept me moving ahead when I was stuck in something crucial and his motivational words and my spirits high, always. I love you dad, as always I did and as I always will.

Tea bush biomass assessment through polarimetric decomposition and semi-empirical modeling

I would like to thank Dr.P.S.Roy (Director, IIRS), Mr.P.L.N.Raju (Group head), Dr.Srivastava (Head, GID), for providing me this platform for learning and developing together with a nice infrastructure and environment.

Further I acknowledge my colleagues in FED for making a peaceful and scientific environment.

The research work would not have been possible without the provision of computing resources by members of Forestry and Ecology division at IIRS. Hence once again, my sincere thanks to Prof. S.P.S. Kushwaha for providing me this environment for carrying out the research work.

Deep regards.

TABLE OF CONTENTS

Contents

Title Page	
Abstract.....	(I)
Acknowledgement.....	(II)
Table of Contents.....	(IV)
List of Figures.....	(VI)
List of Tables.....	(VIII)
1. Introduction	11
1.1. Motivation and problem statement	11
1.2. Research Identification	13
1.2.1. Research Objectives	13
1.2.2. Research Sub-Objectives.....	13
1.2.3. Research Questions	13
2. Literature Review	14
2.1. Description of Tea:	14
2.1.1 History of tea :.....	14
2.1.2.The Assam Tea Plant:.....	14
2.1.3 Requirements:.....	15
2.1.4 Biomass:	15
2.1.5 Biomass estimation using optical data:	17
2.1.6 Application of SAR techniques:	17
2.2. The microwave remote sensing:	19
2.2.1 Polarization :.....	19
2.2.2 The scattering matrix :.....	19
2.2.3 Covariance Matrix :.....	20
2.2.4 Coherency Matrix :.....	20
2.3. Polarimetric Decomposition :	21
2.3.1 Coherent decomposition.....	21
2.3.2 Incoherent decomposition	23
2.3.3 The Durden model:.....	25
2.4. The Freeman -II Model:	26
2.5. Yamaguchi Decomposition Technique:	26
2.6. Multilooking:	26
2.7. Previous work done:	27
3. Study Area	29
3.1. Description:.....	30
4. Materials and Methodology	34
4.1. General:.....	34
4.2. Data used:	34

4.3.	Collection of Field Inventory data:	36
4.4.	Multilook setup:	40
4.5.	Covariance matrix:	40
4.6.	Decomposition:	40
4.7.	Workflow:	40
4.8.	Approach:	42
4.9.	Conversion of slant range to ground range:	43
4.10.	Generation of amplitude images:	43
4.11.	Data conversion :	43
4.12.	Linear to decibel conversion:	44
4.13.	The Coherency Matrix :	44
4.14.	Standard Error:.....	45
4.15.	The Decomposition Model:	45
4.16.	Biomass from the SAR images:	46
4.17.	The working:	46
4.17.1	Training:	46
4.17.2	Validation:	46
5.	The Water Cloud Model	47
5.1.	The Water Cloud Model	47
5.2.	The Two way transmissivity:	49
5.3.	The Modelling theory:	50
5.3.1	The condition of symmetry:	52
5.3.2	The Scattering Models:	52
5.3.3	WCM:	53
6.	Results and Discussion	55
6.1.	General:.....	55
6.2.	Model Training:	55
6.3.	Field data collection:	56
6.4.	Retrieval of the Model Parameters:	56
6.5.	Distribution of the tea bushes in the study area:	59
6.6.	Retreival of Stem Volume using scattering:	60
6.7.	Relation between Biomass and the area of sector:	61
6.8.	Relation between Volume and Height of the bush:	62
6.9.	Relation between the modelled volume and the Ground measured volume:	63
6.10.	Above ground biomass retrieval using the backscatter:	65
6.11.	Relation of volume and biomass:	67
6.11.1	Relation between volume scattering and biomass:	67
6.12.	Relation between bush canopy and biomass:	68
6.13.	Relation between total backscatter and the modelled backscatter:	68
6.14.	Relation between the backscattered component values:	69
6.15.	The model evaluation:	70
6.16.	Discussion:	71
7.	Conclusion	73
7.1.	General:.....	73
7.2.	Recommendations	76

8.	References:	78
9.	Appendix A.....	84
9.1.	LIST OF SYMBOLS	84
10.	Appendix B.....	86
10.1.	LIST OF SYMBOLS	86

LIST OF FIGURES

Figure Number		Page Number
Fig. 2.1	Two component scattering from a forest showing the main contributors as (a) vegetation layer scattering and double bounce from the ground trunk interaction or (b) vegetation layer scattering and direct ground return.....	26
Fig. 3.1	The Sarusarai Tea Estate, Jorhat, Assam (location of the study area in India).....	29
Fig. 3.2	The Sarusarai Tea Estate, Jorhat, Assam. (Google Earth).....	30
Fig. 3.3	The Sarusarai Tea Estate. (a) the tea bushes, (b) freshly pruned bushes, (c) the division in sectors through roads, (d) women pruning the tea bushes, (e) tea bushes before pruning, (f) pruned bushes of the tea estate.....	32
Fig. 3.4	The Sarusarai Tea Estate. (g) freshly pruned bush, (h) the new plants (saplings), (i) part of the garden with new plantation.....	33
Fig. 4.1	The study area: (a) the Google Earth image showing sample plots, (b) the sector wise distribution of the study area.....	38
Fig. 4.2	Flow diagram of the methodology.....	41
Fig. 4.3	Multi look complex image.....	42
Fig. 6.1	The Sarusarai Tea Estate (The Pauli RGB generated(a), surface scattering image(b), volume scattering image(c)).....	57
Fig. 6.2	Relation between the total backscatter and the modelled volume.....	58
Fig. 6.3	Relation between the total backscatter and the measured volume per plot.....	58
Fig. 6.4	Distribution of the tea bushes in the study area pertaining to their type...	59
Fig. 6.5	Percent area wise distribution of the sectors. The legend denotes the sector number.....	59
Fig. 6.6	Relation between the stem volume and the modelled biomass.....	60
Fig. 6.7	Relation between the stem volume and the height of the bush.....	62

Fig. 6.8 Relation between Ground measured volume and modelled volume.....	64
Fig. 6.9 Relation between the modelled volume and the ground measured volume (a) the non-pruned bushes, (b) the pruned bushes.....	64
Fig. 6.10 Relation between ground measured biomass (X-axis) and the modelled biomass (Y-axis).....	65
Fig. 6.11 Relation between ground measured biomass (X-axis) and the modelled biomass (Y-axis).The non-pruned bushes(a), and the pruned bushes (b).....	66
Fig. 6.12 Relation between the modelled biomass and the ground measured volume.....	67
Fig. 6.13 Relation between the modelled biomass and the backscattered volume.....	68
Fig. 6.14 Relation between the bush canopy diameter and the modelled biomass.....	68
Fig. 6.15 Relation between the total backscatter and the modelled backscatter.....	69
Fig. 6.16 Relation between the volume scattering and the surface scattering.....	69

LIST OF TABLES

Table Number		Page Number
Table 4.1	ALOS characteristics.....	34
Table 4.2	PALSAR characteristics.....	35
Table 4.3	The sectors and the year of plantation.....	39
Table 6.1	Biomass and area of the sectors.....	61

1. INTRODUCTION

1.1. Motivation and problem statement

Tea is one of the most important beverages not only in India but across the whole world. As far as India is concerned, it is the most consumed beverage across the country. Not only consumption but India is the largest producer of tea in the world and hence tea contributes to the economic hold and domain of the country thus also helping earn foreign exchange. The production and export of tea has declined over the past few years. This may be because of many reasons. Tea is one of the biggest industries in India but is in a consolidation phase. It's production and quality is decreasing from what it used to be few years ago. However export and domestic use is on hype. Meanwhile, Indian tea is experiencing competition from similar industries of China, Sri Lanka, Kenya and Bangladesh, Indonesia. As per numerical values, tea production and export decreased in northern part of country and also at some parts the prices went low [9]. Tea plantations are of an average of 5 to 6 feet (approx. 1.6 m) tall; much smaller than trees, but generally they are kept at a height of 3 to 4 feet (approx. 1m) so as for ease of plucking. Biomass estimation is important to measure the changes in the vegetation structure, productivity, biomass management, etc. These factors help in the better tea bush productivity and yield. This definitely increases the quality and quantity of the tea production. Biomass estimation through remote sensing has been a long time investigation interest.

Optical imaging technologies are widely used for this cause. However, the optical sensors operate at wavelengths of the order of $1\mu\text{m}$ [7], thus they give the surface information of the vegetation/biomass. For the biomass information we also need other parameters like bush height, number of culms/bush, number of bushes/unit area (field inventory data).The limitation is that optical data cannot detect inside the canopy, hence canopy structure information cannot be retrieved by them. To overcome these limitations, radar remote sensing is considered as the best option. In the past, research has been done to estimate vegetation biomass by retrieving information through Synthetic Aperture Radar (SAR) [2] [3]. Active radar remote sensing uses the microwave region of electromagnetic spectrum (1.3mm to 1m), as its energy source to obtain the information on earth features. The penetration capacity of the radar waves is high. The properties of microwaves (long wavelengths) allow beam to penetrate through clouds, vegetation and even through ground (dry soils). Day and night imaging is possible giving opportunity to obtain the continuous coverage by the microwave satellites. The bands available to extract the information are X, C, L, P bands. The P band radar data is not available from satellite till date but only from the aircraft. The X band, with short wavelength (2.4 to 3.8 cm and 12.5 to 8 GHz frequency) and small penetration depth, only gives information of the canopy surface. The C band (3.8 to 7.5 cm and 8 to 4 GHz frequency) gives the information of the complete canopy as it can penetrate more in the canopy. However these cannot give any information regarding the canopy-soil interactions. For this reason L band (15 to 30 cm and 2 to 1 GHz frequency) has

been used. L band can penetrate deep into the canopy and can retrieve information of the ground also. The L-Band has been used in previous researches/studies regarding forests [44][57]. At L-band, scattering also occurs within the vegetation canopy volume, thus carrying information about parameters of major relevance to vegetation inventory.

In polarimetry, the object information is retrieved through the polarized EM (electromagnetic) wave which comprises of different polarizations. For satellite data polarimetric radar uses single frequency, and has four different polarizations (HH, HV, VH, and VV). Here HH and VV are co-polarized terms and HV and VH are the cross-polarized terms. In case of Quad-polarized SAR or fully-polarimetric SAR data, all the four polarization channels are used, which means more information about the target. Polarimetric SAR systems collect the 2×2 scattering matrix containing values for all the four polarization channels, and hence complete polarimetric scattering information(amplitude and phase), at every imaged pixel [1]. This allows the polarization synthesis of any combination of H and V. Decomposition technique is used to separate different scattering mechanisms. Presence of moisture in soil or vegetation increases radar reflectivity. Plants have large surface area and often have high moisture content therefore they are good reflectors of radar energy [7]. Because of complex geometry of plant canopies, description of interaction mechanism is difficult [11], and hence the need for models arises.

Broadly categorising, there are three classes of models: physical basis, semi-empirical and empirical. Validation of physical models is difficult because the backscatter measurements together with many complex measurements of the plant structure and material properties are required. And these models cannot be validated against extensive datasets. In the case of empirical models, they may be good for general use for vegetation, but due to greater complexity of canopy structure, may not be practically of very much use [11]. However it has limitations like they have no theoretical basis and are based on experimental and observed data [12]. On the other hand, semi-empirical models are suitable and promising for practical use (hence called “user models”). It is not always necessary to account for the effect of all the factors involved. Some variable values vary from species to species. So, there is no general model type. The values for empirical parameters are often determined experimentally and model validation is required in some cases [11].

Different kinds of semi empirical models have been developed like the Water Cloud Model (WCM), Forward models [56], etc. The forward models, in order to estimate radar backscatter based on modelling the canopy, and interaction with EM energy, require many inputs [2]. The basic flow of the forward models is that they have a straight linear flow. Such models take input, process it and the result is the output. Estimating some subsets of these parameters is a difficult problem due to mismatch of number of observable (radar data) versus number of geophysical parameters. Retrieval of parameters describing the geometry of the canopy structure, or the dielectric properties of branches, and leaves is a difficult problem. On the other hand using forward models to predict backscatter values is also difficult because overall backscatter may not be sensitive to significant variations in vegetation properties. If one kind of scattering dominates the return, subtle changes in the other interaction may not be evident in full polarization signature.

The problems faced are in single polarized, information for only one channel is available and dual polarized, prominently used in many previous studies, uses two channel information (e.g., HV, HH). This does not give complete per pixel information of the amplitude and phase [8]. It is difficult to retrieve backscatter amount of radiation from ground and tea bushes. The canopy structure information supports in biomass estimation. The volume scattering was not considered for the semi-empirical model for tea bushes. The decomposition of scattering matrix can give surface scattering and volume scattering values for per pixel..

1.2. Research Identification

To estimate the biomass, the structural information of the canopy is needed to be extracted. An increased biomass level means increased backscattering coefficient. To get the complete per pixel information of the amplitude and phase, quad-pol data scores over dual-pol. The decomposition technique is proposed to be used which gives information of each scattering mechanism separately (e.g. surface, volume). A semi empirical model is to be used to retrieve the information for the volume scattering. This model will be a two layered model as in case of tea plantations. This is because the double bounce scattering information is about negligible in case of tea bush plantations. Hence surface and volume scattering will be considered. Finally retrieval of the biomass is to be done with the WCM parameters and the accuracy assessment of the model.

1.2.1. Research Objectives

The main objective is to retrieve biomass of tea, utilizing semi empirical model through polarimetric decomposition technique.

1.2.2. Research Sub-Objectives

1. To retrieve backscatter contributed by ground and vegetation from single resolution SAR cell;
2. To retrieve the WCM model parameters;
3. To estimate above ground biomass of tea plantations (bushes); and
4. Accuracy assessment of modelled above ground biomass.

1.2.3. Research Questions

The above research objectives can be met by subsequently answering the following research questions:

1. How to utilize the scattering matrix elements for coherency matrix based decomposition to extract volume scattering and surface scattering information from polarimetric SAR data?
2. What is the relation between vegetation scattering and ground scattering for L-band fully polarimetric tea plantation data?
3. What is the use of scattering mechanism and modelling to retrieve the WCM parameters?
4. How to retrieve above ground biomass with the help of the WCM parameters?
5. What will be the accuracy of the modelled above ground biomass in comparison with the field measured above ground biomass?

2. LITERATURE REVIEW

2.1. Description of Tea:

2.1.1. History of tea :

The word tea is derived from *t'e* of the Chinese Fukien dialect. In Cantonese tea is known as *Ch'a*. This name reached India, Russia, Middle East and Iran. Tea drinking originated in China and as mentioned in an ancient Chinese dictionary. Drinking tea as a beverage started in the sixth century as medicinal decoction prepared by boiling tea leaves. Slowly it attracted the attention of the government and a duty was levied on it in 783 A.D. Even the Arabian travellers visiting China in the ninth century spoke of tea as the country's common beverage. The first book on tea "*Ch'aChing*" (Tea Classic) was published in 780 A.D. by Lu Yu. The Dutch introduced tea in Europe in the mid seventeenth century. In 1947, facilitated by a sea route between India and East, the Portuguese started large-scale tea trading. The Dutch bought tea from Japan and the first consignment of tea was shipped in 1610 A.D. Within 100 years it became highly popular in the British Isles followed by America and in the colonies of the British Empire. [26].

2.1.2. The Assam Tea Plant:

Robert Bruce first saw the plant growing wild in the hills of Rangpur (near present Sibsagar) in 1823, the then capital of Assam. After the death of Robert Bruce in a Burmese war, the plant was supplied to his brother C.A.Bruce by Singhpo chief. The seeds were planted in Bruce's garden at Sadiya and some were sent to Commissioner Jenkins at Gauhati. Few leaves were sent to the Indian Botanical Garden at Howrah. In 1834, Lord William Bentinck, appointed a tea committee for commercial cultivation of tea in India. The committee secretary G.J.Gordan, went to China in 1836 to bring tea seeds to India. These seeds were used to raise nurseries in the Indian Botanical Garden, and the plants were sent to Upper Assam, Dehradun, Kumaon, and the Nilgiri Hills. The first samples of the Assam tea, were sent to Calcutta in 1836, which received favourable comments. This was forwarded to London in 1838 which was auctioned in London on 10th January 1839.

The tea plant description as accepted by the botanists does not appear in the Chinese literature. The generic name *Camellia* has been derived from Kamel, George Joseph Kamel, a German missionary stationed in the Philippines, who wrote about plants found in Asia in the latter half of the seventeenth century. In 1935, the botanical congress in its Amsterdam session, decided to unite the two genera, *Thea* and *Camellia*, into a single genus, *Camellia*. A committee decided "*Camellia sinensis (L.) O. Kuntze*" as technically correct name of the plant [26].

2.1.3. Requirements:

Tea requires hot and humid climate. Tea also requires well-drained fertile acidic soil on high lands having a good depth and the pH within 4.5 to 5.5. The organic matter should be greater than 2%. Ground water table depth should be 90 cm or above for good growth of tea. Sufficient rainfall in the winters and early spring is essential for high yield. Ambient temperature between 13°C and 32°C is good for tea growth. With increasing distance from the equator, the length of the growing season decreases. To raise nursery, sandy loam soil is the best. In the middle of the last century, seed was used to grow tea. A simple, cheap and rapid vegetative cloning method was developed in the third and fourth decade of the last century at Toklai, which made it possible to vegetatively multiply the plant. The first cloned tea was released in 1949 to the world. There are about 30 clones of tea available till date. Later Toklai started breeding clonal seed stocks. The planting of the tea plant requires utmost care and should be planted correctly. This results in quick and vigorous growth of the tea bush. There are different types of planting:

1. Pit planting
2. Trench planting
3. Bheti planting
4. Stump planting

Tea estates have shade trees which are very important and play a vital role in the growth of the tea bushes. In NE the temperature rises up to 30°C during the main tea growing season i.e. June to October, shade trees improve health and productivity of the tea bushes. Excessive heat and light radiation is reduced. This is the main benefit of shading trees. The other positive aspects of the shade trees are soil moisture prevention in dry winter months, addition of organic matter by leaf fall, decrease of red spider incidence [36].

2.1.4. Biomass:

Biomass, in general refers to the above ground and the below ground living mass that can be trees, vines, shrubs, roots or the dead mass of the fine and coarse litter present in the soil. The collection of the below ground biomass is rather difficult and henceless concentrated upon. Most of the earlier researches are associated with the estimation of the above ground biomass (AGB)[17]. Forest biomass is defined as the total amount of the above ground living organic matter in vegetation expresssed as oven dry tons per unit area.it is also defined as the living plant material mass per unit area. In general biomass measurement is carried out by the techniques mentioned below[12]:

- a. Harvest mapping technique (destructive sampling)
- b. Non-destructive sampling
- c. Airborne/spaceborne remote sensing data
- d. Estimation using models

a. Harvest sapling technique (destructive sampling):

This technique involves vegetation removal as per a pre defined sample unit of the forest area. The vegetation are seperated into the components like the foliage, branches, stem, twigs, etc. This completely depends on the reason and requirement of the survey. Firstly, the fresh weight is taken and then the samples of the vegetation are oven dried. After drying the samples are weighed again to get the weight after oven drying. Thereafter, biomass is estimated over unit area using appropriate factors.

b. Non-destructive sampling:

The destructive sampling is often not practically applicable and is also time consuming and often not economical as compared to other techniques. Hence the non-destructive sampling method is one of the most widely used. In this technique, various kinds of regression equations are used for the estimation of biomass. These can be linear, quadratic, exponential, allometric, logarithmic, etc. Such methods are time-effective, cheaper than destructive sampling methods and also possible for inaccesible areas where there is large amount of hetrogenety in the vegetation type. However to study the heterogenous vegetations and inaccessible areas, the remote sensing techniques are much helpful.

c. Airborne/Spaceborne remote sensing data:

The remotely sensed data scores over other methods of data collection and processing in the way that they are synoptic in nature, various resolutions like spatial and temporal are available and also the wide variety of formats assist to process the data as desired. there are many at times requirment to estimate the biomass of an area where field survey is difficult or the area is totally inaccessible. In such cases remote sensing is the only source of primary data extraction.

d. Estimation using models:

The above methods of sampling utilize one or the other model for the estimation of above ground biomass and retreival of the parameters. 32 models of the vegetation canopy has been reviewed by [63]. Four categories of models have been recognised by [64] for the vegetation and microwave interraction. They are: Empirically derived models, Dielectric slab model, Random media models and Lossy scatter models.

The methods utilizing GIS and ancillary data are often difficult due to unavailability of good quality ancillary data, environmental conditions impacts of AGB accumulation and indirect relationships between ancillary data and AGB [17]. This is the reason of non-application of GIS based methods widely for extensive AGB estimation. Most of the empirical models have the limitation that they cannot be applied to a wide variety of vegetation due to locally collected datasets and the dataset dependency of the model. On the other hand the semi empirical models consider both the theoretical and the observational values. The semi empirical models have been implemented for forests due to their characteristics earlier by [51][70][12]. AGB has been estimated for broad leaved species and thus the productivity rates. The difference between present and estimated past diameter distribution together with allometric equations were incorporated to estimate the productivity rate [21]. Remote sensing data has been used to estimate the forest biomass. The estimation of the biomass also depends upon the ground truth

verification and biomass equations required to calculate the biomass dependant on the variables thus recorded or measured. In this regard allometric equations are very much needed and thus help in calculating the biomass. Still these works pertains to the biomass calculation of the forest areas. Although study has been done on above ground biomass woody vegetation, yet there is still deficiency of equations and calculating methods for lower height plants such as bushes both in India and in Europe [25][57].

2.1.5. Biomass estimation using optical data:

Optical remote sensing so far has considered the leaf chemistry/structure to, first, measure the vegetation indices like the NDVI and second to use the technique of modelling i.e. NDVI-biomass related to AGB [58]. Optical sensor data for AGB estimation has been categorised based on spatial resolution based on three categories [17]. The estimation of above ground biomass of the himalayan region forests of Uttar Pradesh has been done by [18] and constructed empirical regression model relating total AGB, basal cover and crown cover[18]. The relationship between Landsat-TM data and plot wise field data was established using k-nearest neighbour estimation technique[19]. Few techniques were summarized by [17] for extraction of the individual tree information by using spatial resolution images. IKONOS data has been used to estimate the AGB of vegetation areas in Africa by [65]. For the past few decades remote sensing using optical data has been an effective tool for vegetation assessment in India [20]. Finer spatial resolution together with multispectral characteristics are still considered as one of the best sources for vegetation AGB estimation. In some cases when the field sampling is expensive and time-consuming, biomass is often estimated using biophysical relationship between biomass and crown diameter. In such cases structural variables are considered. Thus biomass is estimated from the biophysical relationships e.g. the crown diameter [22]. Lidar data has been used to estimate tree crown diameter. This followed with measuring individual tree [23]. However this was implemented on the deciduous, coniferous and mixed stands of varying age.

2.1.6. Application of SAR techniques:

In the electromagnetic spectrum the most commonly used wavelength for vegetation mapping and monitoring is of the spectrum of the visible light. However a large amount of work has been done in the infrared spectrum and radio wavelengths. The major drawback of the optical wavelengths is that they cannot penetrate the thick cloud cover, atmospheric dust and hence retrieval of the data beneath the cloud cover is almost impossible. The optical remote sensing is also much dependant on the solar illumination. These limitation are crossed utilizing radar which gives independence both from the the solar illumination problem and also from the cloud problem. Microwave imaging can be done both day and night and they have enough capability to penetrate the clouds, moisture present in the environment and the atmospheric dust. Further, the radar modes operate at multiple combination of polarizations. Thus the observation is possible at any period of time and without much hindrance.so the canopy can be monitored and even with polarimetric SAR data bands the structural vegetation parameters can be retrieved [12].

The earlier studies show that radar backscatter values show strong positive relationship with biomass, height of vegetation [60][61][67]. Vegetation biomass has been related with radar data and it has been recognised that the backscatter from the P band has strong corelation with vegetation biomass (specially forests) as compared to C,X band in airborne data [12]. Study has been done using X,C, L bands from airborne data to evaluate SAR use for estimating above ground biomass of savanna woodlands [57] . Thus different bands are suitable for different type of vegetation. The backscatter of radar at high frequencies (C- and X-bands) is dominated by scattering in the crown layer (branches and foliage) of the canopy, whereas backscatter at lower frequencies (P- and L-bands) is dominated by scattering of woody biomass components (trunks and branches) [4]. Single and dual polarized SAR sensors have already proved their ability by capturing information about earth features, independent of weather. Even then problems exist in these systems to obtain fully structural information from the back scattered signal. Using fully polarimetric SAR systems, this problem was solved to an extent, by obtaining the information from every SAR resolution cell, at a single time using four polarization channels. Fully polarimetric SAR systems collect the 2×2 scattering matrix containing values for all the four polarization channels, and hence complete polarimetric scattering information, at every imaged pixel [1]. This allows the polarimetric synthesis of any combination of H and V. Since dual-pol polarization mode takes only half of the scattering matrix, dual-pol reduces the data processing requirements and the information content in the imagery [1]. In the dual polarization the information retrieved from the dual channels are not sufficient, hence quad polarization data is used which has more no of channels which gives more information.[8]. The dual-pol modes collect only half of the full scattering matrix, either (HH, VH) or (VV, HV). This reduces both the data processing requirements and the information content of the polarimetric imagery. In the past research has been done with two layer radar backscatter model [6][2]. Biomass estimation using SAR has been a well-practiced method for the past few years. The water cloud models with two and three parameters have been used earlier [5][7][16]. The polarimetric decomposition technique used in previous investigations and research considered single bounces, double bounces (ground and canopy) [6].

To understand and estimate the biomass, many models have been developed over time. A model was developed by [66] to understand the backscattering of the layered vegetation. It could explain the ground scattering, crown-ground interaction, crown scattering, trunk and trunk ground interractions to some extent. [67] developed a two layered model to understand microwave scattering mechanismfrom vegetation. Also, the radar data potential to estimate stand parametres and and the AGB has been worked out earlier [59][69]. Generally, the conventional radar remote sensing methods which include backscattering amplitudes evaluation to quantify the forest biomass are limited to biomass levels below 150 tons/ha.. There have been attempts in past to use the forest height for the estimation of the above ground biomass in temperate beech and spruce forests [24].

2.2. The microwave remote sensing:

In microwave remote sensing, the electromagnetic spectrum region of approximately 1mm to 1.3m is utilized. These wavelengths are beamed using antennas rather than lenses and hence is called radar remote sensing.

Microwaves are not “micro” waves. In fact the longest microwaves are about 2,500,000times longer than the shortest light waves [7]. Microwaves are longer wavelengths and so are not vulnerable to atmospheric scattering like the optical waves. They are capable of penetrating the atmosphere. Different wavelengths of microwave can have different penetration level. Compared to optical wavelengths, they can penetrate haze, light rain, snow, and even cloud and smoke. Thus, the desired information or data can be collected at any time of the day. There are two types of microwave remote sensing; (i) active and (ii) passive [33]:

1. Active microwave remote sensing: this kind of remote sensing is done basically when the sensor implied uses its own energy i.e. emits and receives the energy emitted by itself. This kind of remote sensing assists in the day as well as in the night time. Active sensors like the radar, generate their own illumination via transmitting microwave radiation pulses and thus recording and measuring the reflected signal from the area of interest generally the wavelengths greater than 3 cm are used which can penetrate the atmosphere [33].
2. Passive microwave remote sensing: passive remote sensing uses passive sensors(or radiometers)which measure the microwave energy reflected from the target on which solar rays are incident or thermal emission radiated energy. The frequencies facilitate measurements of the atmosphere, ground or rain. The radiometers used to measure the emission from the atmosphere are known as microwave sounders [33].

2.2.1. Polarization :

Polarization describes the path of the tip of the electric field vector of an electromagnetic wave. Polarization can be described in terms of the pattern carved out in space by the tip of the vector at a fixed time, or can be described how the tip of the vector appears to move in time at a fixed location. Polarimetric information is necessary in both active and passive remote sensing. It is composed of two polarization states combined together to form the actual polarization. And these states must be orthogonal i.e each state must be pure and do not contain elements of the other. Which means horizontal polarization will not contain any “vertical component” and vice-versa [35]. In case of EM radiation conventionally the electric field vector direction is taken as the direction of polarisation [33].

2.2.2. The scattering matrix :

The polarimetric measurements of the echoes are orthogonal measurements and is defined as a scattering matrix. It is an array of complex numbers which describe the polarization transformation of incident wave over a scatterer to the backscattered polarization. It can also be referred as a transformation matrix. The stokes vector is not the most efficient way to characterize the data because there are two quantifiable polarization measurements. In general the scattering matrix is [33]

$$S = \begin{pmatrix} S_{VV} & S_{VH} \\ S_{HV} & S_{HH} \end{pmatrix} \quad 2.1$$

where the subscript refers to the pair of transmitted and received pulses. Here the linear horizontal is represented by H and the linear vertical by V . Every element of the matrix i.e. S_{pq} is a complex number describing the amplitude and the phase of the p transmitted and q received pulses. To compute this matrix, the orthogonal radar polarizations are used. The advantage of the scattering matrix is that the relationship between incident and scattered wave field is described in contrast to the Stokes Vector.

$$\begin{pmatrix} E_v^s \\ E_h^s \end{pmatrix} = \frac{e^{-ik_0 r}}{R} \begin{pmatrix} S_{VV} & S_{VH} \\ S_{HV} & S_{HH} \end{pmatrix} \begin{pmatrix} E_v^i \\ E_h^i \end{pmatrix} \quad 2.2$$

Radar systems measuring the amplitude and phase of all four terms of this scattering matrix are termed as “fully polarimetric”. In the real world the condition of reciprocity can be involved, i.e. $S_{HV} = S_{VH}$. This is practically convenient because the cross polarization terms will be of much lower intensity as compared to the co polarized terms, hence are likely to be more influenced by the background or instrument noise. Hence, for accuracy and reducing the noise, the average is considered [33], i.e.

$$S_{HV} = \frac{1}{2}(S_{VH} + S_{HV}) \quad 2.3$$

2.2.3. Covariance Matrix :

To characterize the similarity of polarimetric channels, few more matrices are defined from the target vector such as the covariance and the coherency matrices. It generally records the statistical interrelationships between different channels, the covariance matrix being the most common. It is denoted by C , and is generated by the matrix multiplication of target vector with its complex conjugate [33]

$$C = k \cdot k^{*T} \quad 2.4$$

Where, $*$ denotes complex conjugate and T denotes the transpose. So:

$$C = k \cdot k^{*T} = \begin{bmatrix} S_{VV} \\ S_{HH} \\ S_{HV} \end{bmatrix} \begin{bmatrix} S_{VV}^* & S_{HH}^* & S_{HV}^* \end{bmatrix} = \left\langle \begin{bmatrix} |S_{VV}|^2 & S_{VV} S_{HH}^* & S_{VV} S_{HV}^* \\ S_{HH} S_{VV}^* & |S_{HH}|^2 & S_{HH} S_{HV}^* \\ S_{HV} S_{VV}^* & S_{HV} S_{HH}^* & |S_{HV}|^2 \end{bmatrix} \right\rangle \quad 2.5$$

The $\langle \dots \rangle$ brackets denote ensemble averaging, i.e. averaging over a set of pixels. The covariance matrix as compared to the scattering matrix is just another way of expressing individual properties of received signal in power domain.

2.2.4. Coherency Matrix :

The Coherency matrix, T , is a real valued matrix conveying relation between scattered signals in the channels of a radar polarization thus describing information about the scatterers present in the scene. It can be considered as an alternative to the covariance matrix but is formed by the Pauli target vector [33].

$$T = k_p \cdot k_p^{*T} \quad 2.6$$

where;

$$K_p = \frac{1}{\sqrt{2}} \begin{bmatrix} S_{hh} + S_{vv} \\ S_{hh} - S_{vv} \\ 2S_{hv} \end{bmatrix}$$

thus,

$$\mathbf{T} = \frac{1}{2} \begin{pmatrix} \langle |S_{HH} + S_{VV}|^2 \rangle & \langle (S_{HH} + S_{VV})(S_{HH} - S_{VV})^* \rangle & 2\langle (S_{HH} + S_{VV})S_{HV}^* \rangle \\ \langle (S_{HH} - S_{VV})(S_{HH} + S_{VV})^* \rangle & \langle |S_{HH} - S_{VV}|^2 \rangle & 2\langle (S_{HH} - S_{VV})S_{HV}^* \rangle \\ 2\langle S_{HV}(S_{HH} + S_{VV})^* \rangle & 2\langle S_{HV}(S_{HH} - S_{VV})^* \rangle & 4\langle |S_{HV}|^2 \rangle \end{pmatrix}$$

When the scattering matrix elements are arranged as a vector, the coherency matrix is the expected value given by T . Here the reciprocity is valid. In this case k can be written as $[S_{xx}+S_{yy}, S_{xx}-S_{yy}, 2S_{xy}]^T$, the three elements referred to as Pauli components of the signal to be analysed. After multiplication with the complex conjugate, T reduces to a $3x3$ matrix. Number of sample values are usually averaged to estimate the coherency matrix. This results in a lower resolution image with reduced noise.

2.3. Polarimetric Decomposition :

Polarimetric decomposition is an approach to parameterize the information contained in a polarimetric radar measurement. A combination of idealized scatterers can characterize polarimetric responses [33]. The response from a target may be described as a combination of double bounce(diplane), single bounce, volumetric scattering.

2.3.1. Coherent decomposition

Coherent decomposition expresses the measured scattering matrices in the form of combinations of the scattering responses of the simpler objects [34]. The scattering matrix is decomposed to understand the coherent (pure) targets. The radar cross section contain coherent sum of scatterers. This is because the radar resolution cell size is greater than wavelength of radar system. However the scattering matrix cannot characterize the partially polarized waves. In general, a direct analysis of the scattering matrix, to infer physical properties of the scatterer under study is difficult. Hence the second order derivatives of the scattering matrix, popularly the coherency matrix is considered. The response of every one simple object (canonical object):

$$[S] = \sum_{i=1}^k c_i [S]_i \quad 2.7$$

c_i indicates the weight of $[S]_i$ and k is the number of scattering matrices. The decomposition exposed here is not unique because there is possibility of infinite sets in which $[S]$ can be decomposed. Pauli, the Krogager and the Cameron decomposition are the types.

The covariance matrix represents the resolution cell group's properties. It is generated by the matrix multiplication of the lexicographic scattering vector with its transpose. Coherency matrix is generated, by multiplying the pauli basis scattering vector to its transpose. Covariance and coherency matrices are hermitian positive semi definite matrices and hence are quite

similar in properties and have same Eigen values. They are related by unitary similarity transformation matrix. The radar senses the geometrical characteristics of the objects whose information is provided by these matrices. Hence they can be decomposed into components which represent underlying scattering types [35].

2.3.1.1. Pauli Decomposition:

The Pauli decomposition expresses the measured scattering matrix in Pauli basis i.e. if the conventional orthogonal linear basis is considered, the Pauli basis is a four 2x2 matrix[34].

$$[S]_a = \frac{1}{\sqrt{2}} \begin{bmatrix} 1 & 0 \\ 0 & 1 \end{bmatrix} \quad 2.8$$

$$[S]_b = \frac{1}{\sqrt{2}} \begin{bmatrix} 1 & 0 \\ 0 & -1 \end{bmatrix} \quad 2.9$$

$$[S]_c = \frac{1}{\sqrt{2}} \begin{bmatrix} 0 & 1 \\ 1 & 0 \end{bmatrix} \quad 2.10$$

$$[S]_d = \frac{1}{\sqrt{2}} \begin{bmatrix} 0 & -1 \\ 1 & 0 \end{bmatrix} \quad 2.11$$

Since reciprocity applies in monostatic systems configuration and hence $S_{hv} = S_{vh}$. The matrix $[S]_a$ corresponds to the scattering matrix of a sphere, a plate or a trihedral and is referred to as single or odd bounce scattering. The second matrix $[S]_b$ represents a scattering mechanism characterized by double bounce or even bounce. This is because the returned wave polarization is mirrored with respect to the incident wave. Here a complex coefficient of scattering is involved represented by β and $|\beta|^2$ represents the scattered power by this type of targets:

$$\beta = \frac{S_{hh} - S_{vv}}{\sqrt{2}}$$

The third matrix corresponds to the scattering mechanism of a diplane oriented at 45° and refers to those scatterers which return the orthogonal polarization e.g. the volume scattering (produced by the forest canopy). Here γ represents the contribution of $[S]_c$ and $|\gamma|^2$ represents the scattered power by this type of scatterers [34].

2.3.1.2. The Krogager Decomposition:

Krogager proposed to factorize the scattering matrix as the combination of the responses of sphere, a diplane and a helix. The diplane and the helix component present orientation angle θ . In this type of decomposition there are five coefficients($\varphi_s, \theta, k_s, k_d, k_h$) and an absolute phase φ . This φ contains about the scatterer. The absolute phase φ contains information about the scatterer but its value depends on the distance between the radar and the target hence is not relevant. The parameters φ and k_s characterize the sphere component. The phase parameter gives information about the orientation angle of the diplane and the helix component.

2.3.1.3. The Cameron Decomposition:

The Cameron decomposition factorizes the measured scattering matrix based on reciprocity and symmetry. It states that a reciprocal target can be decomposed as a sum of two components.

$$\vec{S} = A \left[\cos \tau \vec{S}_{sym}^{max} + \sin \tau \vec{S}_{sym}^{min} \right] \quad 2.12$$

Further, the Cameron decomposition provides a classification scheme on basis of factorization of measured scattering matrix. Few other models are the radiative transfer model which assumes that particles scatter independently. The leaves are modelled as randomly oriented distributed discs and needles. This model considers only one polarization. The backscatter coefficient is retrieved by using first order solution of radiative transfer equation [34].

The electric field vector of the transmitted pulse can be vibrating(polarized) either in horizontal or vertical plane. After striking the terrain, the reflected pulse generally has the same polarization as the incident/transmitted pulse. The reflected energy is recorded as like polarized (or parallel polarized) images i.e. HH (horizontal transmit, horizontal received) or VV (vertically transmit, vertically received). A part of the returning energy is depolarized by the surface of the terrain and thus deflected vibrates in various directions. This happens because of the multiple reflections at the surface.

2.3.2. Incoherent decomposition

Among decompositions eigen value based technique is popular. It provides entropy and average target scattering mechanism. This works on basis on eigen value analysis of coherency matrix. The Eigen value provides statistical independence between target vectors. The scattering matrix characterises only the coherent or pure scatterers. However the distributed scatterers are not characterised by this matrix from polarimetric perspective. Such scatterers can be characterised due to presence of speckle noise. Therefore, second order polarimetric representation is used to analyse the distributed scatterers. The second order descriptors are the 3×3 covariance $[C_3]$ and coherency $[T_3]$ matrices. These two are equivalent. The direct analysis of the coherency and covariance matrix for study of scatterers is difficult due to complexity of scattering process. The main objective behind using the incoherent decompositions is to separate the covariance $[C_3]$ or coherency $[T_3]$ matrices as combinations of second order descriptors corresponding to simpler canonical objects. This presents an easier physical interpretation. The decomposition theorems can be expressed as[34]

$$\langle [C_3] \rangle = \sum_{i=1}^k p_i [C_3]_i \quad 2.13$$

$$\langle [T_3] \rangle = \sum_{i=1}^k q_i [T_3]_i \quad 2.14$$

Here p_i and q_i are the coefficients of the components in $[C_3]$ or $[T_3]$. Here the components $[C_3]_i$ or coherency $[T_3]_i$ are independent or in a restrictive way, orthogonal and need not correspond to pure targets. The types are Freeman, Huynen and the Eigenvector-Eigenvalue decompositions.

2.3.2.1. Freeman Decomposition:

The Freeman model decomposes the covariance matrix as the contribution of three scattering mechanisms [34].

Volume scattering: The canopy scatter is modelled as a set of randomly oriented dipoles.

Double bounce scattering: This is the scattering modelled by dihedral corner reflectors. This is also known as even bounce scattering.

Single bounce scattering: This is modelled by first-order Bragg surface scatterer. Also known as surface or odd bounce scattering [2].

The volume scattering from vegetation is modelled considering it as randomly oriented thin dipoles. The scattering matrix of an elementary dipole is

$$[S] = \begin{bmatrix} R_h & 0 \\ 0 & R_v \end{bmatrix} \quad 2.15$$

For a thin dipole the above reduces to

$$[S] = \begin{bmatrix} 1 & 0 \\ 0 & 0 \end{bmatrix} \quad 2.16$$

Considering the set of randomly oriented dipoles, the covariance matrix can be modelled as

$$[\mathcal{C}_3]_v = f_v \begin{bmatrix} 1 & 0 & 1/3 \\ 0 & 2/3 & 0 \\ 1/3 & 0 & 1 \end{bmatrix} \quad 2.17$$

where, f_v corresponds to the volume scattering. The covariance matrix presents rank 3 hence volume scattering is not characterized by single scattering matrix of a pure target.

Another component of the model is the first order Braggs scattering (i.e. the surface scattering). The covariance matrix comes out to be

$$[\mathcal{C}_3]_s = f_s \begin{bmatrix} |\beta|^2 & 0 & \alpha \\ 0 & 0 & 0 \\ \alpha^* & 0 & 1 \end{bmatrix} \quad 2.18$$

where: f_s corresponds to the surface scattering and $\beta = R_h/R_v$.

The Freeman decomposition expresses the total covariance matrix as

$$[\mathcal{C}_3] = [\mathcal{C}_3]_v + [\mathcal{C}_3]_d + [\mathcal{C}_3]_s \quad 2.19$$

The scattered power of the volume, double bounce and surface scattering component are as follows

$$P_v = \frac{8f_v}{3} \quad 2.20$$

$$P_d = f_d(1 + |\alpha|^2) \quad 2.21$$

$$P_s = f_s(1 + |\beta|^2) \quad 2.22$$

The scattered power is used to generate to a RGB image to visualize the polarimetric information into a single image. The total scattered power is maintained. This is also called the span image. Hence, Span is:

$$SPAN = P_v + P_d + P_s \quad 2.23$$

2.3.2.2. Surface scattering:

It is defined as scattering from the interface between two dissimilar media, such as atmosphere and the earth's surface. For a homogenous medium, (i.e. if the volume scattering is considered as absent), characterized by a relative dielectric constant ε_r , for a small surface roughness compared to radar wavelength, the scattering mechanism is specular. In such kind of scattering, the reflection of the incident wave and its transmission through the surface is given by Snell's law. If a wave is incident at an angle θ , a portion of the energy will be reflected at an angle θ and a portion refracted at an angle θ' , [32] where,

$$\theta' = \sin^{-1}(\sin \theta / \sqrt{\varepsilon_r}) \quad 2.24$$

2.3.2.3. Bragg's scattering:

Considering a homogenous medium, (i.e. no volume scattering) with an rms height variation less than $\lambda/8$, then the scattering can be described using Bragg's model. The Bragg's model states that dominant backscattered energy arises from the surface spectral components resonating with incident wave. At wavelengths (w), the backscattered return will be strong.

$$\Lambda w = n\lambda/(2\sin\theta) \quad n=1,2,3,\dots \quad 2.25$$

The dominant return is for the wavelength when $n=1$. For steep incident angles, there is a combination of Bragg and specular scattering. Sometimes for Bragg surface the specular scattering is dominant. This depends on local slope. The incident wave has two components; a scatter component due to local slope and point scatterer component depending on the roughness of the surface. Thus the resultant backscatter curve is a combination of these two curves which is a function of local incidence angle [32].

2.3.3. The Durden model:

The microwave energy incident on the vegetation is backscattered. To understand them L-band microwave scattering model was developed, to simulate microwave backscatter value. The consideration is the uniform distribution of scatterers. The branches were considered as upper layer and were modelled as dielectric cylinders randomly oriented. The lower layer in case of trees was modelled as layer consisting of tree trunks considering randomly oriented dielectric cylinders. The lower layers were modelled as tree trunks again as randomly oriented dielectric cylinders. Brags surface was considered for the ground. The double bounce and ground backscatter was also considered. Further, a two layer model of Durden model was also developed. For the upper layer vertical dielectric cylinders was considered randomly oriented cylinders to model the trunks and needles for the leaves. The basic disadvantage of these models was some of them had more number of input than the number of output. Few of them were mathematical and was difficult to relate them with the physical scattering models (the physical models consider the scattering on the interaction of electromagnetic waves with the vegetation parameters).

2.4. The Freeman –II Model:

The Freeman-II model came in the year 2007[2], which is basically an extension of the work done in Freeman-Durden model[16]. The scattering mechanisms considered were surface scattering

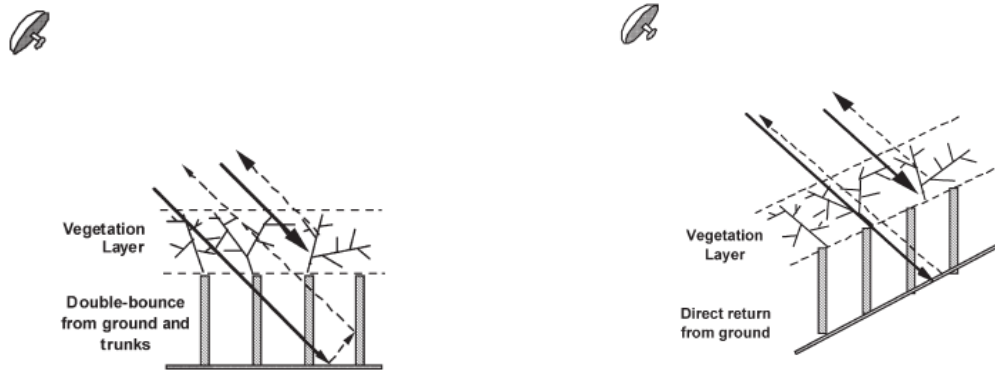


Fig. 2.1 Two component scattering from a forest showing the main contributors as (a) vegetation layer scattering and double bounce from the ground trunk interaction or (b) vegetation layer scattering and direct ground return [2].

scattering and double bounce scattering from ground and trunks. The canopy scatters from a reciprocal medium having azimuthal symmetry. The double bounce scatters from a pair of orthogonal surface having different dielectric constants. The model has been applied on a tropical forest. The model has been used to understand the ground trunk double bounce scattering present in the data and it varies as a function of incident angle. The attenuation coefficient also plays a key role in the forward models and is related to the canopy density. This mechanism has the capability to model variety of canopy structures. The figure shows the two component scattering mechanism.

2.5. Yamaguchi Decomposition Technique:

The Freeman Durden three component model was further extended by introducing the Helix component as a fourth component [29]. The covariance matrix approach is used to deal the non-reflecting symmetric scattering case [43]. It deals with the reflection symmetry condition that the co-polarized and cross-polarized correlations are close to zero. The helix scattering is accounted for the co-polarized and the cross-polarized correlations generally appearing in the urban areas scattering and disappear in the natural distributed scatterer. A modification of the volume scattering matrix in the decomposition technique has been considered. The modification yields asymmetric matrices which can be adjusted to measurement data with $\langle |S_{HH}|^2 \rangle \neq \langle |S_{VV}|^2 \rangle$, where $\langle \dots \rangle$ brackets represents the ensemble average in the data processing.

2.6. Multilooking:

Multi-looking generally reduces the effect of speckle from the SAR images. It is a process of compressing angle or azimuth resolution which leads to better visualization of the image [35]. Multi-looking is a kind of image correction which reduces effects of speckle in radar images. It shows the averaging degree of SAR measurements during data formatting. The process of multi-looking is performed in the frequency domain. Thus, it helps in speckle reduction and makes computation easy [34].

2.7. Previous work done:

Study has been done on different models and decomposition techniques using scattering models. In general four types of scattering is considered. They are surface scattering, double bounce scattering and volumetric scattering. The attempt started with [16] who used three scattering mechanisms to polarimetric SAR observations. The three mechanisms included scattering from the canopy from a cloud of randomly oriented dipoles, double bounce scattering from ground and tree stem and Bragg's scatter from rough surface. The composite model shows discrimination between flooded and non-flooded forests, forested and deforested areas. The scattering from the three mechanisms can be estimated for pixel clusters in the Pol-SAR images[16]. The model fits scattering behaviour for bare soil at P band. The surface scatter is quite prominent in C band. The farmlands show volume scatter in the C band. Thus longer wavelength penetrates the short vegetation and thus the backscatter is mainly due to the underlying ground.

The vegetation signature and the oriented urban areas on decomposing with the volumetric scattering are difficult to distinguish with respect to radar direction of illumination. Thus rotation of the coherency of the coherency matrix has been accounted for thus considered [29]. The Freeman-Durdan model had some drawbacks [2]. A two component decomposition model was proposed by [2]. He came up with a better two component scattering model. He has also shown that a priori knowledge of the vegetation height, an estimate for the attenuation coefficient of the canopy can be obtained directly from the multi incident angle polarimetric observations. This attenuation coefficient (β) is related to the canopy density. However, in the previous paper there was a scarcity of reliable geophysical parameters extracted from radar data. No success has been achieved through combining polarimetry and interferometry techniques to recover tree heights. In the new paper focus is on extracting information purely from polarimetric backscatter data [2]. A two component model would yield a good description of the scattering signatures in most cases (two scattering terms are dominant). For volume scattering it has been considered that that the radar return is from randomly oriented, very thin, cylinder-like scatters. Several simplifying assumptions have been made to derive the second order statistics of the scattering matrix (the coherency matrix). It considered double bounce and volume scattering. The model shows canopy scattering from randomly oriented scatterers. The azimuthal symmetry has been considered. However the model gives better results only for forests. Most of the imaged area, the HH-VV phase difference shows ground-trunk double bounce interactions. The canopy scatter has low HV backscatter but the correlation was strong between HH and VV and hence can be considered the model failure to describe the scattering from particular surface [2].

A semi-empirical model i.e. water cloud model proposed by [28], considers that vegetation is composed of 99% of air by volume thus canopy is modelled as water cloud. The vegetative matter contains the droplets of the water cloud. The reason behind this kind of modelling is that the available moisture in the canopy shows larger dielectric constant than dry canopy and air. The WCM considers that the water content is randomly distributed throughout the canopy [28]. The WCM model has the backscatter values as the parameters in the model. The backscatter values show saturation effect with short wave microwave [12][37][38].The modelling of the backscatter as a function of stem volume was conducted using L-Band WCM by Santoro et. al (2006). As per the study, the stem volume retrieval is effected by weather conditions [5]. The volume scattering of Pol-SAR data for the estimation of vegetation

parameters by [39] shows the variation of volume coherence with polarization. Also, the length of the coherence line is influenced by the vegetation height [39].

The Yamaguchi model shows the use of the coherency matrix to deal with the symmetric scattering [40]. The results obtained are almost the same as when the covariance approach was implemented. For volume scattering a randomly oriented dipole model was considered. A transact was chosen on the image. The power plot derived through the coherency matrix coincided with the covariance matrix approach. The study proves the identity of the results of the four component decomposition result approach based on the coherency and the covariance approach [40]. In the generation of the coherency matrix from a randomly oriented cloud of particles the copular scattering coefficients and the cross polar terms are uncorrelated. The single scattering system has zero entropy; circular polarization is rejected by the choice of sphere. The single scattering terms are rejected and thus multiple scattering terms are left behind [41]. The polarimetric SAR interferometry used by [1] to invert the SAR data with random volume over ground model. Forest height –biomass allometric equations were used to generate biomass of the forest from forest heights. A physical extraction of the forest parameters was used (allometric equations) to estimate the biomass. These often include stem counting, crown size and height estimations. Correct biomass estimation is possible by unconditional use of height biomass allometry [42].

An extension of the Freeman-Durdan model was achieved by the introduction of an asymmetric volume scattering covariance matrix that depends on the relative backscattering magnitude between HH and VV. Considering the surface, double bounce, volume scattering respectively, the model is effective for POLSAR images P-L-C band. The modification of the volume scattering matrix has been done regarding backscattering magnitudes. The uniform distribution of the density function yields the covariance matrix for the volume scattering of the randomly oriented dipoles. Emphasis has been laid on the covariance matrix. The matrix elements do not change, with the change in the individual scattering matrix. Adjustment can be made to the asymmetric matrix to the relation with the scattering matrices. The volume scattering suggests that HH component dominates over VV component for L-Band [43].

Another model suggested by [44] describes the volume scattering contributions when the media does not follow azimuthal symmetry case in case of the observed backscatter. The model is adjustable to the polarimetric radar data which considers higher HH sensitivity against VV terms to the canopy. An improved scattering power decomposition method for four components has been presented by [45] in which a proper volume scattering model has been utilized for polarimetric SAR data. Differentiating between vegetation and oriented buildings is difficult in the decomposed images. This is because the volume scattering due to vegetation is assigned the HV component. The study proposes the extension of the volume scattering model considering the physical scattering.

3. STUDY AREA

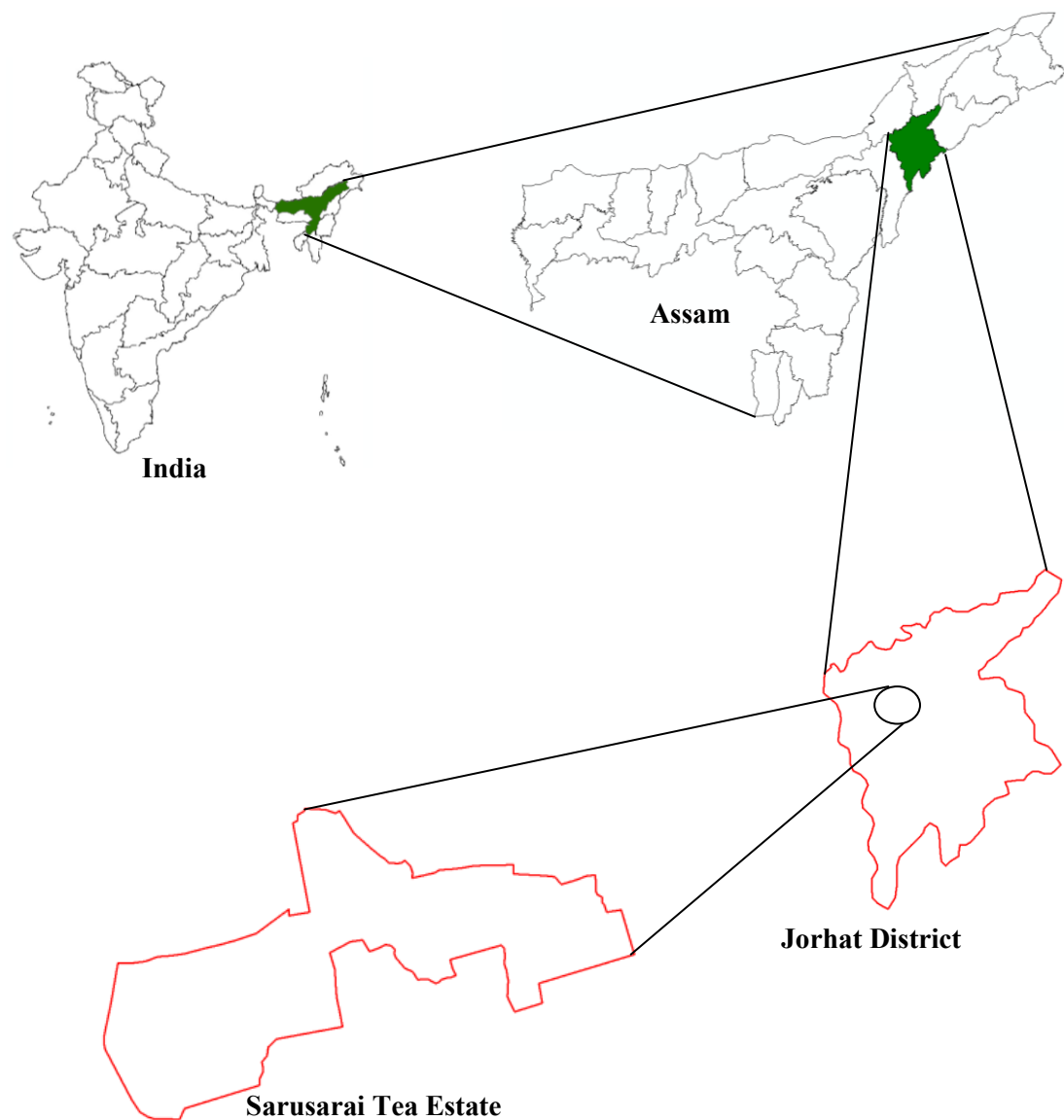


Fig.3.1:The Sarusarai Tea Estate, Jorhat, Assam(location of the study area in India).

3.1. Description:

Jorhat (26.75°N 94.22°E) is the 2nd largest city after Guwahati in Assam. It is situated 307 km north-east of Guwahati at 116 m elevation from mean sea level. As per the history of Assam, Jorhat was established as a capital in the late 18th century by the Ahom Dynasty-Tunkhungia during its decline. The name has its origin from jor (meaning merger) and hat (meaning markets); the two parallel markets being Chowkihat and Macharhat on the eastern and western banks of the river Bhogdoi. Jorhat is also known as the cultural capital of Assam province. It is also one of the major business hubs of Assam. The city is located amidst tea estates and has world famous tea research centre, The Tea Research Association (TRA) at Toklai which is only one of its kinds in the world. Jorhat Provincial Railway, a narrow gauge train service was started by the British in 1885 for exporting tea and timber from Jorhat to other parts of the world as major trade commodity. It is during this period that tea industry was rapidly established.

There are five tea estates around Jorhat which occupy considerably large area. They are Sarusarai tea estate, Honwal tea estate, Lohpohia tea estate, Moabondha tea estate and the Sangsuwa tea estate. The study area, the Sarusarai tea estate (STE) is located close to the National Highway 37 at only few kilometres from Jorhat airport at Rowriah. The area covered by the Sarusarai tea estate (Lat: 26.29° - 26.95° N and Long: 94.03° - 94.47° E) is approximately 2 km^2 . Fig.3.2 shows Google Earth image of the Sarusarai tea estate. The image was accessed on 16th January, 2012 at 09:00 hours.

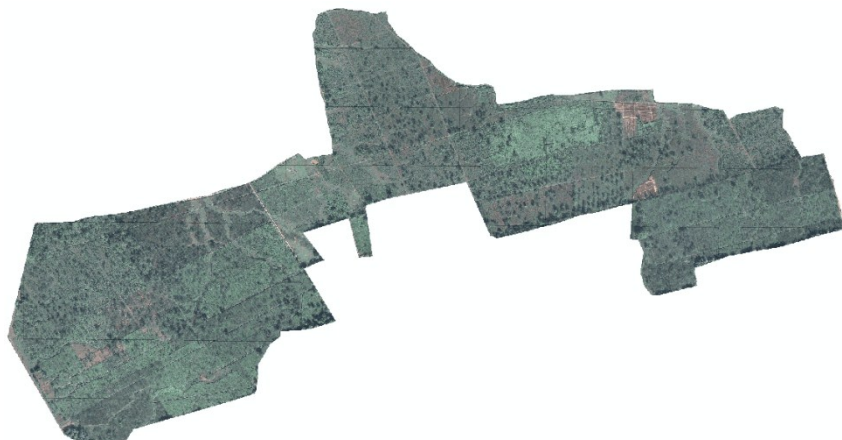


Fig.3.2: The Sarusarai Tea Estate, Jorhat, Assam. (Google Earth).

The average tea bush height in the area as also in STE is $\sim 1\text{m}$. The low height is preferred for ease of plucking the tea leaves. The STE is divided into 38 sectors. Each sector was planted during a particular period. This dates back to the sixties and seventies. Every three year the bushes are pruned to maintain the productivity. Bushes are uprooted and removed when they become unproductive due to a host of reasons including bush age, disease outbreak, etc. The bushes are pruned sector-by-sector. After pruning, chemicals are sprayed over the pruned bush to protect it from the infection and pests. The complete garden has a properly distributed network of canals for water drainage. The tea plants do not tolerate water logging

although high rainfall is a necessity. Drainage system, therefore, is carefully developed and low lying areas altogether avoided. In some sectors tea bushes had leaves during field survey. Few newly planted sectors have hardly any appreciable tea bush canopy. The tea bushes in the sectors are not equally dense in all parts of the garden. In some sectors the tea bushes are sparsely populated with higher inter-bush gaps.

The STE also has a nursery of their own. The saplings, grown in the nursery, are transplanted in the tea estate. The tea saplings need less water and hence, water supply is always regulated. In some sectors, tea bushes are very dense, with hardly any space left for leaf plucking. This is basically a function of the bush age, older the plantation lesser is the space for movement. Few sectors are so scarcely populated that in critical cases there are one or two bushes in 25 m^2 area. This is due to the removal of the tea bushes or sometimes the wild boars, dig the bush out while searching for the underground tubers. In such cases new saplings are planted in between the old bushes. This makes the bush cover in that region heterogeneous with respect to the year of plantation and thus in relation to the age-wise distribution of the bushes. This probably affects the backscatter of the microwave energy.



Fig.3.3: The Sarusarai Tea Estate. (a) the tea bushes, (b) freshly pruned bushes, (c) the division in sectors through roads, (d) women pruning the tea bushes, (e) tea bushes before pruning, (f) pruned bushes of the tea estate.



(g)



(h)



(i)



(j)



(k)



(l)

Fig.3.4: The Sarusarai Tea Estate. (g) freshly pruned bush, (h) the new plants (saplings), (i) part of the garden with new plantation, (j) & (k) uneven gaps between bushes, (l) mature tea bushes in STE nursery.

4. MATERIALS AND METHODOLOGY

4.1. General:

This chapter is divided into two parts. The first part deals with the data source followed by the detailed research method adopted for this study. The method also includes the conversion of data in lexicographic and Pauli format for the purpose of generation of coherency matrix. The method includes generation of coherency matrix. This has further been used as input parameter for Freeman-II model to generate surface and volume scattering and also generation of power images. The values, thus obtained, are used in the water cloud model to estimate the biomass of the vegetation (in this case tea plantations).

4.2. Data used:

The data used in this project is ALOS (Advanced Land Observing Satellite), Japan PALSAR (Polarimetric Phased Array L-band Synthetic Aperture Radar) fully polarimetric L Band data. PALSAR is a fully polarimetric remote sensing instrument, with HH or VV single polarization, dual polarization (HH+HV or VV+VH), or polarimetric (HH+HV+VH+VV).
ALOS characteristics

Table 4.1: ALOS characteristics[15].

Launch Date	Jan.24,2006
Launch Vehicle	H-IIA
Launch Site	Tanegashima Space Centre
Spacecraft Mass	Approx. 4 tons
Generated power	Approx. 7KW (at end of life)
Design Life	3-5 years
Orbit	Sun-Synchronous Sub-Recurrent
	Repeat Cycle : 46 days, Sub Cycle : 2 days
	Altitude : 691.65km(at equator)
	Inclination : 98.16 deg.
Attitude Determination Accuracy	2.0×10^{-4} degree(with GCP)
Position Determination Accuracy	1m (offline)
Data Rate	240 Mbps (via Data Relay Technology Satellite) 120 Mbps (Direct Transmission)
On-board data Recorder	Solid state data recorder

Table 4.2: PALSAR characteristics[15].

Mode	Fine	Scan SAR	Polarimetric(Experimental Mode)*1
Center Frequency	1270 MHz(L-Band)		
Chirp Bandwidth	28 MHz	14 MHz	14 MHz, 28 MHz
Polarization	HH or VV	HH+HV or VV+VH	HH or VV
Incident Angle	8 to 60 deg.	8 to 60 deg.	18 to 43 deg.
Range Resolution	7 to 44 mm	14 to 88 m	100 m(multi look)
Observation swath	40 to 70 km	40 to 70 km	250 to 350 km
Bit Length	5 bits	5 bits	3 or 5 bits
Data Rate	240 Mbps	240 Mbps	120 Mbps, 240 Mbps
NE Sigma Zero *2	<-23dB (Swath Width 70 km) <-25dB (Swath Width 60 km)		<-25 dB <-29 dB
S/A *2,*3	>16dB (Swath Width 70 km) >21dB (Swath Width 60 km)		>21 dB >19 dB
Radiometric Accuracy	Scene:1dB/orbit; 1.5 dB		

*1 represents due to power consumption

*2 represents valid for off nadir angle

34.3 deg. (fine mode)

34.1 deg. (Scan SAR Mode)

21.5 deg. (Polarimetric mode)

*3 represents S/A level may deteriorate

due to engineering changes

in PALSAR.

Method:

The following section explains the method adopted during the course of this research.

4.3. Collection of Field Inventory data:

The complete tea garden is divided into approx. 38 sectors. Not all sectors have the same type of bushes. The bushes vary not only in age, but also in the built. Few have large canopy, others have small canopy. The stem size and the number of branches often denote the years it has crossed. To some extent pruning limits the lateral expansion of the bush. Stratified random sampling method was adopted for field data collection. The basic reason for this choice is the varying age of the bushes as well as the planting density. The age of the bushes was considered as per the year of plantation provided by the STE management. Most of them were planted between 40s to 80s.

A field visit was made to collect tea bush biophysical data. This included tea bush canopy geometry (shape and size/spread), bush density, bush height, number of branches per bush, etc. Generally the tea estates in Jorhat have tendency of keeping orderly cultivation of the tea bushes. Different types of tea bushes were stratified using Google imagery of 1m spatial resolution through following steps:

1. Classification of the tea bushes depending upon bush growth stage.
2. Random sampling was done in these strata. At least three sample plots per stratum were laid. By random sampling, the idea is the plots were selected randomly within the strata. Thus attempt has been made to cover each and every sector so that all kind of bushes are sampled.
3. Sample plot size considered was 5m x 5m. In each such plot, the number of bushes was counted. The physical parameters were measured. The bush parameters being tea bush height, area covered by bush, number of branches and twigs. Inter canopy distance was also measured. A total of 160 sample plots were measured.

Samples of bush collected from the field were weighed and fresh weight was noted. These samples were then oven-dried to estimate the dry weight.

The tea bushes sampled consisted of pruned, non-pruned bushes and also the saplings. The total area covered is 151.14 ha. The measurement of different parameters was taken. These included recording of GPS coordinates, girth of stem, stem height, height of bush, no. of primary branches, no. of secondary branches, no. of tertiary branches, girth of primary and secondary branches, canopy spread and inter canopy distance. From this data, stem volume and above ground biomass was generated. The literature reviewed at Forest Research Institute (FRI), Dehradun and Tea Experimental Station (TRA), Toklai showed the unavailability of allometric equation for *Camellia Sinensis*. Hence the stem volume and the biomass were generated using basic regression equations. The field inventory data already records the girth and height values. The basic way of progress is the volume of the branches, stem and twig is calculated using volume equation, considering them as cylindrical volume.

Thus, the volume (V) is:

$$V = \pi r^2 h \quad 4.1$$

where; r^2 = radius of the stem/branch/twig, h = height of the stem/branch/twig

The radius of the stem/branch/twig is calculated from the girth measured:

$$G = 2\pi r \quad 4.2$$

i.e. $r = \frac{G}{2\pi} \quad 4.3$

where; G = girth of the stem/branch/twig

Assuming the bushes to be identical, the total volume of the sample plot is the product of the number of bushes in the sample plot and the volume of a single bush i.e.:

$$V_p = V_b * n \quad 4.4$$

where; V_p = total volume of the sample plot

V_b = total volume of a single bush

n = total no. of bushes in a sample plot

Tea wood volume in each sector was calculated separately. The total volume of a sector is estimated using the area of the sector. The sector-wise volume was calculated using following formula:

$$V_s = \frac{v \cdot x}{25} \quad 4.5$$

where; V_s is the total volume of a particular sector

The total volume of the tea estate (i.e. study area) (\mathcal{V}) is:

$$\mathcal{V} = \sum_{i=1}^n (V_s)_i \quad 4.6$$

The biomass of the bush (B) was calculated as the product of the volume of the bush (V_b) and the specific gravity of tea (ϱ).

$$B = V_b * \varrho \quad 4.7$$

The biomass for each and every sector is calculated separately. The total biomass of the tea estate (B_{Tot}) was calculated as:

$$B_{Tot} = \sum_{i=1}^n B_i \quad 4.8$$

Fig. 4.1 illustrates the location of the sample sites (160 sample sites/plots) for which field data was collected.

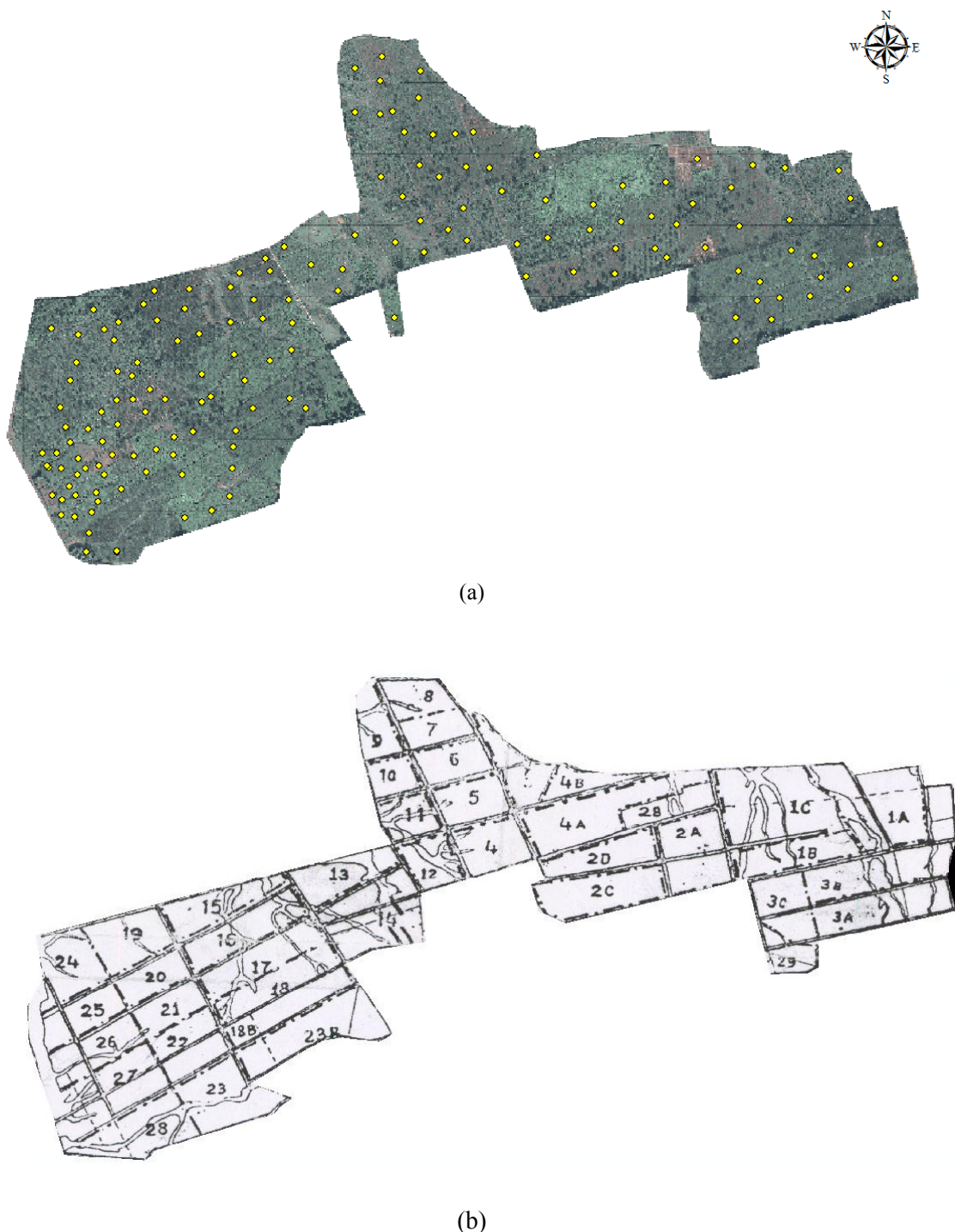


Fig. 4.1: The study area: (a) the Google Earth image showing sample plots, (b) the sector wise distribution of the study area.

Table 4.3:The sectors and the year of plantation

Sec. No.	YOP	Sec. No.	YOP
1.1	1949	10	1961
1.2	1950	12	1964
1.3	1950	13	1970
2.1	1955	14	1970
2.2	1956	15	1969
2.3	1957	16	1969
2.4	1956	17	1969
3.1	1982	18	1969
3.2	1985	19	1965
3.3	1984	20	1966
4	1964	21	1966
4.1	1964	22	1966
4.2	1964	23	1973
5	1960	24	1966
6	1960	26	1969
7	1960	27	1969
8	1955	28	1968
9	1961	29	1980

The above table shows the year of plantation of the individual sector(s). The year determines the age of the plantation. In all there are 27 major sectors. Four sectors are further subdivided to form sub-sectors. They are the first four sectors. The difference between the year of plantation is upto 35 years. The older plantations, in general, have large canopy and few of them have bulky size.

4.4. Multilook setup:

The ALOS PALSAR data is a single look complex mode fully polarimetric data. This SLC image includes the information of the complete polarizations. When a signal is transmitted, it is reflected back. Sometimes the antenna receives more than one responses from different objects on the ground, from a transmitted signal. In such a case, the time difference gives the distance between the objects. This distance is called the slant range and is in the sensor look direction. Because of this slant range distortion, the near range objects appear compressive thus resulting in different azimuth and range direction resolution. So, the effect of this slant range can be reduced by converting slant range into ground range through trigonometric conversions. The process creates ground range images by adding number of looks from the azimuth direction. The available data contains an approximate range resolution of 21m and azimuth resolution of 3m. On conversion of slant to ground range, the single look complex image is used to generate a multilook setup. To make square pixel, the no. of looks considered in the range direction is 1 and in the azimuth direction is 6. Thereby, the resolution in the azimuth direction increases from 3m to 22m. This creates the multilook image. [35]

4.5. Covariance matrix:

The measured quantity in a polarimetric radar is the complex scattering matrix. The received power by the radar is squared magnitude of voltage and is also represented in terms of the covariance matrix [55]. One of the second order derivatives of the scattering matrix is the covariance matrix. The covariance matrix is expressed in terms of lexicographic format. The covariance matrix in this case is a 3x3 matrix with the assumption of the reciprocals.

4.6. Decomposition:

The above created covariance matrix has been used in the Freeman-II decomposition model to decompose for the different scattering mechanisms. The Freeman-II model uses five elements out of nine elements in the covariance matrix as it considers the reflection symmetry condition.

4.7. Workflow:

The complete flow diagram of the methodology is divided into major three parts; the generation of the backscattered images, coherence estimation. The final phase consists of training the model, estimating model parameters and analysis of the results. The model parameters are estimated from the backscatter measurements and the field inventory data.

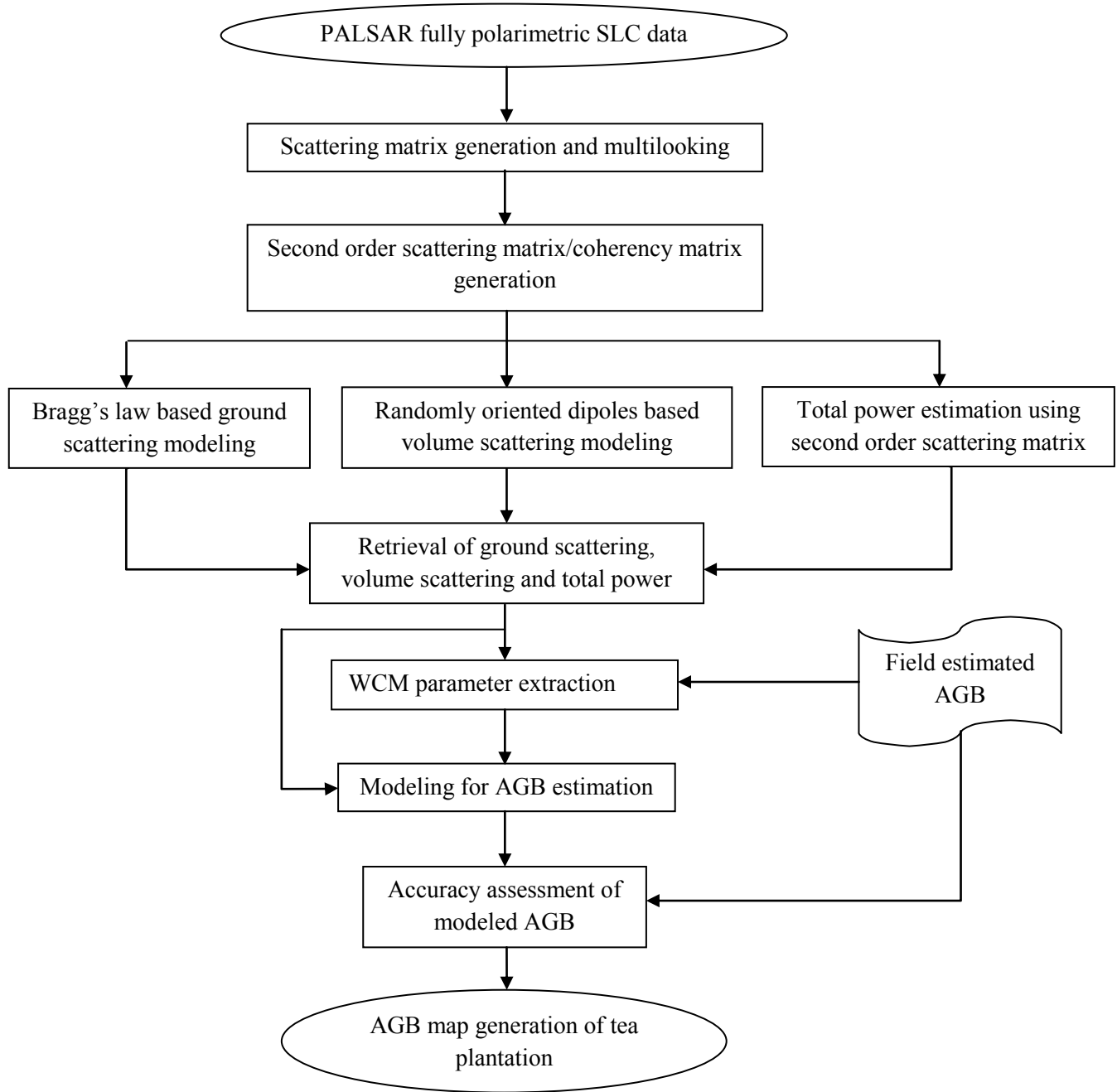


Fig. 4.2. Flow diagram of the methodology

4.8. Approach:

The data provided contains single look complex (SLC) images of quad-polarimetric mode containing the four mode HH, HV, VH, VV information and a header file which contains the information about the images. These images are used for generation of scattering matrices. The scattering matrix is as below.

$$S = \begin{pmatrix} S_{VV} & S_{VH} \\ S_{HV} & S_{HH} \end{pmatrix} \quad 4.9$$



Fig. 4.3: Multi look complex image

The scattering matrix is a 2x2 complex element containing co-polarized information as the diagonal elements and the cross-polarized information as the off diagonal elements.

The multilook image is generally generated for easy visualization of the features on the image. Thus the appearance of the image increases. To create the colour combination of the image, HH+VV was expressed through blue/green, HV+VH through green, HH-VV through red. This is the Pauli's form of expression. The vegetation is depicted in green colour, built up area

in blue and double bounce areas in pink or reddish-pink colour. The vector form of the scattering matrix is expressed in lexicographic basis.

$$K_p = \begin{bmatrix} S_{HH} \\ \sqrt{2} S_{HV} \\ S_{VV} \end{bmatrix} \quad 4.10$$

Reciprocal assumption is considered in the lexicographic representation of the data. i.e. $S_{VH}=S_{HV}$.

4.9. Conversion of slant range to ground range:

The time interval between the radar antenna transmitted signal which is received back by the antenna after undergoing backscattering from the objects of the ground, gives the distance of the object from the radar antenna. When the antenna transmits a signal to the ground and receives two different return signals from the object at two different time (time interval) then the time difference between the two responses helps in determining the object spacing on the ground. Based on this concept, the distance between two objects and the distance of objects from the satellite along the sensor direction look (slant range) is measured by a sensor. Because of this slant range distortion, the near range objects appear compressed relative to the far range resulting in captured image scale variation from near to far range. This distortion is removed by the conversion of slant range to the ground range. The ground range is the horizontal distance along the ground for each corresponding point measured in the slant range. This conversion is done using trigonometrical calculation of ground range using known slant range. The process includes reprojection of single look complex (SLC) data into flat ellipsoid surface from slant range. The SLC data is redistributed in range considering equal pixel spacing.

4.10. Generation of amplitude images:

The PALSAR quad-polarimetric data contains four channels each containing one real and one imaginary channel. In general the first channel which denotes the real component is denoted by "I" and the second component representing the imaginary part is denoted by "Q". These two channels are combined to obtain amplitude image. Thus the composite signal intensity is obtained and resultant image pixels show amplitude values. To generate the amplitude image from the complex SAR image, the square root of the sum of the square of the real and the imaginary component of the complex pixel values for the channels are taken. The pixel values of the amplitude image contain a +ve range of real values. The algorithm is:

$$A = \sqrt[2]{(I^2 + Q^2)} \quad 4.11$$

4.11. Data conversion :

The image to be viewed represents total power received by SAR antenna. This image is the power image. Its pixel values are linearly proportional to the power backscattered by the

imaged areas (scenes) of the antenna. The power image can also be defined as the sum of the square of the real and the imaginary components values of the complex pixel values. This process constitutes the amplitude image to power image conversion. The algorithm considered is:

$$P = A^2 \quad 4.12$$

where; P = pixel values of Power image

A = pixel values of the Amplitude image

The resultant image is the floating point image which represents the amplitude image power and the corresponding pixel values having a positive range of pixel values. When the conversion of a power image pixel is done, if it shows negative value, the pixel value is assigned the value zero.

4.12. Linear to decibel conversion:

The backscatter cross section (σ^o) is expressed on a logarithmic scale i.e. decibel(dB) scale [12]. It is generally represented by the ratio of power levels per unit area. The algorithm used to convert this backscatter cross section from linear to decibel scale is:

$$\sigma_{i,j}^o(\text{dB}) = \log_{10}\sigma_{i,j}^o(\text{linear}) \quad 4.13$$

The lighter pixels in the backscatter image show high backscatter values. This represents the vegetation whereas the relatively dark pixels represent low backscatter values i.e. the ground surface. The high backscatter value pixels result from vegetation scattering which is a kind of rough surface compared to the size of the wavelength of the L-Band. There is high reflectance and less scattering from smooth surface and thus fewer portions of the transmitted signal returns back to the radar antenna. This appears as a dark pixel on the image. The upper surface of the vegetation acts like a rough surface and thus returns high amount of signal to the radar antenna.

4.13. The Coherency Matrix :

The Coherency matrix, T , is generated from the Pauli target vector. The matrix is generated from the product of

$$T = K_p \cdot K_p^{*T} \quad 4.14$$

When the scattering matrix elements are arranged as a vector, the coherency matrix is the expected value given by T . Thus T becomes:

$$C = \begin{pmatrix} S_{HH}S_{HH}^* & \sqrt{2}S_{HH}S_{HV}^* & S_{HH}S_{VV}^* \\ \sqrt{2}S_{HV}S_{HH}^* & S_{HV}S_{HV}^* & \sqrt{2}S_{HV}S_{VV}^* \\ S_{VV}S_{HH}^* & \sqrt{2}S_{VV}S_{HV}^* & S_{VV}S_{VV}^* \end{pmatrix} \quad 4.15$$

Correlation coefficient amplitude:

The amplitude of correlation between the co-polarized terms is calculated [48][35]. This value varies from 0 to 1. The values which are recorded after direct backscatter from the ground (surface) are near 1. The values for volume scattering are still lower. It is as follows [49]:

$$\rho_{HH-VV} = \frac{\langle S_{HH} - S_{VV}^* \rangle}{\sqrt{|S_{HH}|^2 |S_{VV}|^2}} \quad 4.16$$

4.14. Standard Error:

The assumption considered in the PolSAR images is the noise present in the form of exponential distribution [2]. The standard error in this case being:

$$Standard\ Error = \frac{SD\ (span)}{\sqrt{n}} \quad 4.17$$

4.15. The Decomposition Model:

The concept of the Freeman II decomposition is to model the coherency matrix on basis of the two different scattering mechanisms. This helps in estimating the total backscattered power due to the two types of scattering i.e. surface and the volume scattering.

$$C = P_v C_{vol} + P_g C_{sur} \quad 4.18$$

As per the model, the volume scattering and the surface scattering are as follows:

The Volume scattering (V) is:

$$V = f_v \begin{pmatrix} 1 & 0 & \rho \\ 0 & 1 - \rho & 0 \\ \rho^* & 0 & 1 \end{pmatrix} \quad 0 \leq \rho \leq 1; \arg(\rho) = 0 \quad 4.19$$

The Surface scattering (S) is:

$$S = f_s \begin{pmatrix} 1 & 0 & e^{-2j\phi}b \\ 0 & 0 & 0 \\ e^{2j\phi}b & 0 & |b|^2 \end{pmatrix} \quad |b| \geq 1; \arg(b) = 0 \quad 4.20$$

The above model returns the output parameters of volume and surface scattering of power output as:

$$P_v = f_v(3 - \rho) \quad 4.21$$

and,

$$P_s = f_s(1 + |\alpha|^2) \quad 4.22$$

where; P_v = power output of the volume scattering

P_s = power output of the surface scattering

The details of the model used (i.e. the water cloud model) has been provided in Chapter 5.

4.16. Biomass from the SAR images:

The biomass of the tea bushes is estimated from the polarimetric SAR images. The backscatter values are recorded from the processed SAR images. The surface and volume scattering information is generated from the SAR images. The backscattered values for the sample plots are recorded.

4.17. The working:

The collected field inventory data has 160 sample plots and the information is used for generating the biomass. This data is divided into two equal parts; one for validation and one for training. This means the data is divided 80 and 80 sample points. From the first 80 points, the value for the attenuation coefficient is estimated (i.e. ψ). For this the concept of least square approximation is used. (LSA). The value of ψ is used in the model along with the remaining 80 sample values to validate the model. Further, the volume information is generated from the bush physical parameters.

4.17.1. Training:

The model training comprises of two parts. Firstly, the calculation of volume from the field collected data & secondly the generation of surface scattering & volume scattering information from the SAR data. As stated earlier, the ground (field) collected data comprises of tea bush parameters. These parameter values are used to generate the volume of the bushes. The biomass is estimated from the dry weight of the samples. In such a case, the consideration taken is that all the primary branches are identical, all the secondary branches are identical, all the tertiary branches are identical for a bush. Thus, considering all bushes in a plot as identical, the volume per plot has been estimated. On the other hand, the SAR backscatter image is decomposed to retrieve the scattering information, i.e., the surface scattering and the volume scattering backscatter values. The data is then divided into two equal parts for the training and the validation. The first 80 sample plot values are considered for training of the model. Together, the surface scattering, the volume scattering values and the volume information, are utilized to estimate the value of the two way attenuation coefficient (ψ). This is done by the inversion of the water cloud model. The inverted model gives the value of the attenuation coefficient. The least square approximation method is used to estimate the value of the attenuation coefficient. Finally, the value of ψ thus obtained is used in the model to estimate the biomass for the rest of the (remaining 80) sample plots.

4.17.2. Validation:

The validation of the model starts after the generation of the two way attenuation coefficient (ψ). For the validation, again the inverted water cloud model is used. The remaining 80 values for the volume are used. The backscatter value retrieved from the SAR image together with the attenuation coefficient value is utilized to retrieve the value of the biomass, from the model. The biomass obtained from the model, is the biomass retrieved from the SAR backscatter image with the help of the field measured values. This model retrieved biomass is compared against the field estimated biomass.

5. THE WATER CLOUD MODEL

5.1. The Water Cloud Model

The concept of the water cloud model was originally developed by [28]. This concept is basically a relationship developed between the vegetation parameters and the backscatter of the vegetation. As the name suggests, the water cloud model basically means a cloud assumed to be made of water. The basic assumption of the water cloud model (WCM), is that the vegetation is considered as a homogenous layer or medium filled with droplets of water. These water droplets are considered to be spread uniformly over a horizontal plane surface which represents the ground surface. Thus the elements which are responsible for the scattering caused are the water droplets. When energy is incident on the upper layer of the canopy, part of the energy is reflected back to the radar sensor and remaining part of it transmits (penetrates) the lower layer. The energy transmitted to the lower layer is the attenuation by the upper layer (vegetation layer). The model assumes that all scatters have similar properties. This implies that the attenuation cross section and radar cross section remains same for all the scatters. The total backscatter is represented by the incoherent summation of the scattered energy at each layer. Some of the major properties of the water cloud model discussed by [50] are:

1. The multiple reflections are not included. The higher order scatterings i.e. the even bounce mechanisms are not considered.
2. The odd bounce from the surface of ground and the vegetation has been considered.
3. The vegetation has been treated as a homogenous medium. The canopy gaps were excluded.
4. The cloud of the water particles are made up of similar particles and this is considered as a homogenous medium.

In simple terms the Water Cloud Model can be written as:

$$\sigma_{tot}^0 = \sigma_{veg}^0 + \sigma_{gr}^0 \quad 5.1$$

where, σ_{tot}^0 =total observed value of backscatter

σ_{veg}^0 =backscatter of vegetation (in this case, tea bushes)

σ_{gr}^0 =backscatter of ground

A semi-empirical model quite similar to the above one for vegetation canopy modelling using backscatter values of radar was given by [51]. A similar model which shows relation with biomass is [12]:

$$\sigma_{tot}^o = \sigma_{gr}^o e^{-\psi B} + \sigma_{veg}^o (1 - e^{-\psi B}) \quad 5.2$$

Where: ψ = two way attenuation (empirically defined coefficient);

B = Above Ground Biomass; and

$\sigma_{tot}^o, \sigma_{veg}^o, \sigma_{gr}^o$ are as defined above.

Another model given by [52] which was similar to the original water cloud model but based on the WCM itself is:

$$\sigma_{tot}^o = (1 - \eta)\sigma_{gr}^o + \eta[\sigma_{gr}^o T_{tree} + \sigma_{veg}^o (1 - T_{tree})] \quad 5.3$$

where: η = area fill factor.

The above model was given for the total backscatter of the forest. To consider the in between canopy gaps and the fraction of ground covered by the crown of the tree, each and every term of the above model has been weighed by the area fill factor η .

A fraction called sigma nought(σ^o) describes the amount of power backscattered as compared to power of the incident field. It represents the average reflectivity (of a material normalized) as compared to the horizontal ground plane unit area. Also, referred to as the scattering coefficient. The magnitude of the scattering coefficient is a function of the electrical and the physical properties of the target, the SAR systems wavelength and polarization and the modified incident angle by the local slope [46]. The total backscatter σ_{tot}^o , as denoted above, is expressed as the sum of the direct ground scattering from in between the canopy gaps, the direct ground scattering through attenuation by the canopy, direct scattering from the vegetation layer which is irrespective of attenuation.

1. *Ground scattering from the canopy gaps:* the variable σ_{gr}^o represents the direct backscatter from the ground. The term $(1 - \eta)\sigma_{gr}^o$ represents the ground scattering from in between the canopy gaps. The term $(1 - \eta)$ represents the part of ground which is not under cover of the tree crown. Thus this part of the ground is barely exposed to the incoming energy and also offers least hindrance to the backscattered energy. It also shows the canopy gap backscattering contribution. This indirectly also suggests that vegetation is a discontinuous layer.
2. *Ground scattering through attenuation by the canopy:* the term $\eta\sigma_{gr}^o T_{tree}$ represents backscatter from the ground attenuated by the canopy. The attenuating vegetation layer is represented by ηT_{tree} .
3. *The scattering from the vegetation layer:* the term $\eta\sigma_{veg}^o (1 - T_{tree})$ denotes the direct backscattering from the vegetation layer. The term $\eta(1 - T_{tree})$ is the total unattenuated vegetation backscattering.

5.2. The Two way transmissivity:

The two way transmissivity (T_{tree}) expresses the amount of incident EM wave attenuated after passing through the gaps of the canopy. It is represented by the exponential of the product of the two way attenuation per metre and the attenuating layer thickness [51]. Thus:

$$T_{tree} = e^{-\alpha h} \quad 5.4$$

where: α = the two way attenuation per metre;

h = the attenuating layer thickness

here, the attenuating layer thickness is considered to be approximately equal to the tree height.

On the basis of the area fill factor, the two way forest transmissivity can be expressed as [50]:

$$T_{veg} = (1 - \eta) + \eta e^{-\alpha h} \quad 5.5$$

Thus on this basis, the WCM given by Askne et al.(1995)can be rearranged as:

$$\sigma_{tot}^o = (1 - \eta)\sigma_{gr}^o + \eta[\sigma_{gr}^o e^{-\alpha h} + \sigma_{veg}^o(1 - e^{-\alpha h})] \quad 5.6$$

$$\text{i.e. } \sigma_{tot}^o = [(1 - \eta) + \eta e^{-\alpha h}]\sigma_{gr}^o + \eta\sigma_{veg}^o(1 - e^{-\alpha h}) \quad 5.7$$

earlier studies utilized the C-Band which did not include the even-bounce scattering, i.e. the double bounce scattering between the vegetation and ground. The reason being there is strong attenuation in the energy incident on the upper layer of the canopy. Hence, the two way transmissivity (T_{tree}) can be neglected. Thus the T_{veg} can be expressed as:

$$T_{veg} = (1 - \eta) \quad 5.8$$

It can be clearly seen that the WCM can be considered as:

$$\sigma_{tot}^o = T_{veg}\sigma_{gr}^o + \sigma_{veg}^o(1 - T_{veg}) \quad 5.9$$

The two way forest transmissivity can also be expressed as the exponential of the product of the volume of the stem (V)and an empirically defined coefficient (ψ) as given by Pulliainen et al. 1994) [53]:

$$T_{veg} = e^{-\psi V} \quad 5.10$$

The WCM in this case becomes:

$$\sigma_{tot}^o = e^{-\psi V}\sigma_{gr}^o + \sigma_{veg}^o(1 - e^{-\psi V}) \quad 5.11$$

The two way transmissivity in the form of exponential can be explained as:

$$e^{-\psi V} = (1 - \eta) + \eta e^{-\alpha h} \quad 5.12$$

This gives clearly the relation between the stem volume and the attenuating layer thickness (which also pertains to the height of the tree).

5.3. TheModelling theory:

The water cloud model was further worked upon to provide some sort of simplification. Basically the water cloud model consists of two components i.e. the odd bounce scattering or the single bounce scattering. This component explains the interaction between the incident electromagnetic energy and the ground surface. Thus this is also termed as the surface scattering. The surface scattering also takes place from the exposed ground surface in between the canopy gaps. It is represented by σ_{gr}^o or σ_{sur}^o . The second and important component is the vegetation scattering or the canopy scattering. This component explains the scattering behaviour between the incident electromagnetic energy and the canopy of the bushes. Whenever there is energy incident on the canopy, it not only is scattered back but also some part of it penetrates into the lower level. This energy then, has an interaction with the branches and twigs i.e. there is internal reflections (interaction) within the branches and the twigs. Finally this energy is also backscattered to the sensor which is recorded. Hence this is termed as volume scattering. This means the scattering which takes place within the volume (canopy) of the bushes. It is represented by σ_{veg}^o or σ_{vol}^o . The total backscatter is the sum of the backscattering at each individual levels i.e. summation of the surface scattering and the volume scattering. Thus:

$$\sigma_{tot}^o = \sigma_{sur}^o + \sigma_{vol}^o \quad 5.13$$

In case of bushes (in this case tea bushes) the height of the bush is very low. There could be some backscatter due to even bounce scattering which will almost be negligible in this case. Thus the consideration for double bounce scattering has not been taken into account. Instead only surface and volume scattering components have been considered.

The PolSAR images are decomposed for the constituent scattering information. The scattering mechanisms considered in this decomposition technique are the surface scattering and the volume scattering. The approach for the fitting of this model is that the double bounce scattering has been omitted (or set to zero) as there will be negligible or no such prominent interaction. This is because the tea bushes are very short in height and thus the even bounce scattering between the bushes and the ground will not be of much value or importance. However, the canopy scattering (or the volume scattering) will be dominating due to wide spread of the canopy of the bushes in the study area. There are wide variety of canopies present all over the study area. This kind of scattering mechanism helps in modelling different kind of canopies. After examining the HH/VV amplitude and phase ratio, the model fit reveals the present mechanism. The total backscatter model together with the composite scattering matrix, which is the mean of the calculated values, is represented as below:

$$\langle M_{hh}M_{hh}^* \rangle = f_c + f_g \quad 5.14$$

$$\langle M_{hh}M_{hv}^* \rangle = \frac{1-\rho}{2} f_c \quad 5.15$$

$$\langle M_{vv}M_{vv}^* \rangle = f_c + |\alpha|^2 f_g \quad 5.16$$

$$\langle M_{hh}M_{vv}^* \rangle = \rho f_c + \alpha f_g \quad 5.17$$

where: f_c = contribution due to canopy scattering (volume scattering); and
 f_g = contribution due to ground scattering (surface scattering).

Thus to solve for α from above, we get

$$z_1 = \langle M_{hh}M_{hh}^* \rangle = \langle M_{vv}M_{vv}^* \rangle = f_g(1 - |\alpha|^2) \quad 5.18$$

$$z_2 = 2\langle M_{hv}M_{hv}^* \rangle + \langle M_{hh}M_{vv}^* \rangle - \langle M_{hh}M_{hh}^* \rangle = f_g(\alpha - 1) \quad 5.19$$

Further, to get the value of α , the ratio of the above two is taken:

$$z_3 = \frac{z_2}{z_1} = \frac{(\alpha - 1)}{(1 - |\alpha|^2)} = 0 \quad 5.20$$

After separating the real and the imaginary parts we get:

$$(1 - (x^2 + y^2))R_e(z_3) + 1 - x = 0 \quad 5.21$$

$$(1 - (x^2 + y^2))I_m(z_3) - y = 0 \quad 5.22$$

where;

$$x = \left(\frac{R_e(z_3)y}{I_m(z_3)} + 1 \right) \quad 5.23$$

Substituting x in the above equation:

$$\left(\frac{R_e^2(z_3)}{I_m(z_3)} + I_m(z_3) \right) y^2 + (2R_e(z_3) + 1)y = 0 \quad 5.24$$

Thus solving the above quadratic equation we get:

$$y = \frac{-l_m(z_3)(2R_e(z_3)+1)}{|z_3|^2}; \quad \text{or} \quad y = 0 \quad 5.25$$

Now, the imaginary part and the real part of the equation i.e. α, x can be solved. Following that, f_g and f_c can be retrieved. Thus the value of ρ can be calculated.

The contribution to the span P by each of the scattering mechanism is:

$$P = P_c + P_g \quad 5.26$$

which is equivalent to ;

$$|M_{hh}|^2 + 2|M_{hv}|^2 + |M_{vv}|^2 \quad 5.27$$

where;

$$P_g = f_g(1 + |\alpha|^2) \quad 5.28$$

$$P_c = f_c(3 - \rho) \quad 5.29$$

The term α represents the relative phase and amplitude difference between the backscatter terms.

5.3.1. The condition of symmetry:

In the case of symmetricity of reflection, which has been considered in the model, the condition was shown to equalise the scattering coefficient that were measured in two linear polarizaton bases. Correlation will be zero between the co-polarizes and the cross-polarized terms (scattering coefficients). This is shown as [47]:

$$R_e \sigma_{hhvv} = R_e \sigma_{vhvv} = R_e \sigma_{hhvh} = R_e \sigma_{hvvv} = 0 \quad 5.30$$

$$I_m \sigma_{hhhv} = I_m \sigma_{vhvv} = I_m \sigma_{hhvh} = I_m \sigma_{hvvv} = 0 \quad 5.31$$

Thus the covariance matrix for reflection symmetry condition will be [47]:

$$C = \begin{bmatrix} \sigma_{hhhh} & 0 & \sigma_{hhvv} \\ 0 & \sigma_{hvvh} & 0 \\ \sigma_{hhvv} & 0 & \sigma_{vvvv} \end{bmatrix} \quad 5.32$$

Thus the values are [47]:

$$\sigma_{vhvv} = \sigma_{vvvh} = \sigma_{hhhv} = \sigma_{hvhh} = 0 \quad 5.33$$

The above matrix C has been derived, with the zero elements, based on the symmetricity of reflection condition. There has been no reference to the scattering mechanisms. Due to this condition, it is valid for both volume scattering and surface scattering. Finally the covariance matrix can be expressed using element numbers as:

$$C = \begin{bmatrix} C_{11} & C_{12} & C_{13} \\ C_{12}^* & C_{22} & C_{23} \\ C_{13}^* & C_{23}^* & C_{33} \end{bmatrix} \quad 5.34$$

The elements which conclude to zero are:

$$C_{12} = C_{12}^* = C_{23} = C_{13}^* = 0 \quad 5.35$$

5.3.2. The Scattering Models:

The surface scattering or the ground scattering information is retreived based on the Bragg's law [40]. The surface scattering obtained from the coherency matrix elements terms is:

$$f_s = \frac{1}{2} \langle S_{hv} + S_{vv} \rangle^2 - 4 \langle |S_{hv}|^2 \rangle + 2 |I_m \langle S_{hv}^* (S_{hh} - S_{vv}) \rangle| \quad 5.36$$

where f_s is the backscattered amount contributed by the ground surface.

For the information of volume scattering, a randomly oriented dipole model is implemented. The elements of the volume scattering in terms of the coherency matrix elements are extracted. The expression for the output model for the randomly oriented dipole is:

$$f_v = 8 |S_{hv}|^2 - 4 |I_m \langle S_{hv}^* (S_{hh} - S_{vv}) \rangle| \quad 5.37$$

where f_v is the backscattered amount contributed by the vegetation.

Finally the total modelled power with respect to surface and volume scattering is:

$$P = P_s + P_v = f_s (1 + \psi^2) + f_v \quad 5.38$$

5.3.3. WCM:

The semi empirical model which is based on the polarimetric decomposition considers the principles of the water cloud model, which was initially developed by [5][28]. The model is expressed in terms of the elements of the scattering matrix for the surface and volume scattering:

$$P = e^{-\psi B} \left[\frac{1}{2} (|S_{hh} + S_{vv}|^2) - 4(|S_{hv}|^2) + 2|I_m \langle S_{hv}^* (S_{hh} - S_{vv}) \rangle| \right] \\ + (1 - e^{-\psi B}) [8|S_{hv}|^2 - 4|I_m \langle S_{hv}^* (S_{hh} - S_{vv}) \rangle|] \quad 5.39$$

where ψ is the empirically defined coefficient and B is the above ground biomass of the tea plantation (bushes). P represents the total power. The above equation is in terms of the scattering matrix. The total power is the summation of the the surface scattering and the volume scattering weighted by the area fill factor. The power term surface scattering component(P_s) consists the difference of the sum of half the square of the sum of the co-polarized and twice the difference of the imaginary parts of the co-polarized terms and four times the square of the cross-polarized term, weighed by the ares fill factor, i.e.

$$P_s = e^{-\psi B} \left[\frac{1}{2} (|S_{hh} + S_{vv}|^2) - 4(|S_{hv}|^2) + 2|I_m \langle S_{hv}^* (S_{hh} - S_{vv}) \rangle| \right] \quad 5.40$$

The power term volume scattering component (P_v) consists of the difference of eight times the square of the cross-polarized term and four times the difference of the imaginary part of the co-polarized terms weighed by the ares fill factor, i.e.

$$P_v = (1 - e^{-\psi B}) [8|S_{hv}|^2 - 4|I_m \langle S_{hv}^* (S_{hh} - S_{vv}) \rangle|] \quad 5.41$$

From the above equation, upon inversion, the biomass can also be estimated. After inverting the equation, for biomass (B), it can be expressed as:

$$P = e^{-\psi B} \left[\frac{1}{2} (|S_{hh} + S_{vv}|^2) - 4(|S_{hv}|^2) + 2|I_m \langle S_{hv}^* (S_{hh} - S_{vv}) \rangle| \right] \\ + (1 - e^{-\psi B}) [8|S_{hv}|^2 - 4|I_m \langle S_{hv}^* (S_{hh} - S_{vv}) \rangle|] \quad 5.42$$

or, $P = e^{-\psi B} [\text{surface scattering}] + (1 - e^{-\psi B}) [\text{volume scattering}]$

or, $P = e^{-\psi B} [\sigma_{\text{sur}}^\circ] + (1 - e^{-\psi B}) [\sigma_{\text{vol}}^\circ]$

or, $\sigma_{\text{tot}}^\circ = \sigma_{\text{sur}}^\circ e^{-\psi B} + \sigma_{\text{vol}}^\circ - \sigma_{\text{vol}}^\circ e^{-\psi B}$ 5.43

as P is the total power image which is denoted by $\sigma_{\text{tot}}^\circ$. this is also known as the span image.

The surface scattering is represented by $\sigma_{\text{sur}}^{\circ}$ and the volume scattering is represented by $\sigma_{\text{vol}}^{\circ}$ and the empirically defined coefficient is ψ . Considering the above equation for biomass (B),

$$\sigma_{\text{tot}}^{\circ} - \sigma_{\text{vol}}^{\circ} = e^{-\psi B} [\sigma_{\text{sur}}^{\circ} - \sigma_{\text{vol}}^{\circ}] \quad 5.44$$

thus,

$$e^{-\psi B} = \frac{\sigma_{\text{tot}}^{\circ} - \sigma_{\text{vol}}^{\circ}}{\sigma_{\text{sur}}^{\circ} - \sigma_{\text{vol}}^{\circ}} \quad 5.45$$

or,

$$B = -\frac{1}{\psi} \left[\ln \left(\frac{\sigma_{\text{tot}}^{\circ} - \sigma_{\text{vol}}^{\circ}}{\sigma_{\text{sur}}^{\circ} - \sigma_{\text{vol}}^{\circ}} \right) \right] \quad 5.46$$

The above equation (5.46) is retrieved from inverting the water cloud model. This equation gives the biomass of the tea bushes. The equation utilizes the backscattered values obtained from the SAR image and the two way attenuation coefficient as input and provides the biomass as the output.

6. RESULTS AND DISCUSSION

6.1. General:

There are parameters of the water cloud model that are unknown. These are ground backscatter, backscatter from the tea bushes and the two way bush transmissivity. The parameters are retrieved from the measured bush parameters, e.g. stem volume and bush height. This procedure of retrieving the unknown parameters of the model utilising the field inventory and the measured bush parameters is thus the model training. The model has been trained from a set of measurements taken over 80 sites from the 160 sample plots. The resultant output thus received from the model has been validated for the remaining 80 plots out of the 160 sample plots. The backscattered values are obtained from the SAR backscattered image. The parameters of the water cloud model, were extracted from the SAR image which were finally utilized in the model to retrieve the above ground biomass of the tea bushes.

6.2. Model Training:

The unknowns of the water cloud model are estimated with the help of non-linear regression analysis. The method used is least square approximation. According to the least square approximation method, the sum of the squared difference between the backscatter of the vegetation (bushes) measured and the backscatter of the vegetation (bushes) modelled per plot. Let $\sigma_{mea,i}^{\circ}$ represent the measured backscatter value. $\sigma_{model,i}^{\circ}$ represents the backscatter value modelled for every plot. Thus the least square algorithm applied is as follows:

$$\sum_{i=1}^n [\sigma_{mea,i}^{\circ} - \sigma_{model,i}^{\circ}]^2 = min. \quad 6.1$$

From the earlier equation, the modelled vegetation backscatter becomes:

$$\sigma_{model}^{\circ} = \sigma_{sur}^{\circ} e^{-\psi V} + \sigma_{vol}^{\circ} (1 - e^{-\psi V}) \quad 6.2$$

The equation for unknown parameters of water cloud model can be written as:

$$\sum_{i=1}^n [\sigma_{mea,i}^{\circ} - \sigma_{sur,i}^{\circ} e^{-\psi_i V_i} - \sigma_{vol,i}^{\circ} (1 - e^{-\psi_i V_i})]^2 = min. \quad 6.3$$

Thus the normal equation generated from above equation as per applying least square approximation is:

$$\sum_{i=1}^n \sigma_{mea,i}^{\circ} = \sum_{i=1}^n [\sigma_{sur,i}^{\circ} e^{-\psi_i V_i} - \sigma_{vol,i}^{\circ} (1 - e^{-\psi_i V_i})] \quad 6.4$$

where; V_i = the stem volume of the i^{th} plot.

$\sigma_{sur,i}^{\circ}$ = backscattered value from the ground

$\sigma_{vol,i}^{\circ}$ = backscattered value from the bushes(canopy)

6.3. Field data collection:

The field data collected basically comprised of the tea bush physical parameters. The study area was divided into smaller plots each of 5m x 5m area. The measurement comprised of the measurement of the parameters like the bush height from the ground surface, girth of the stem, number of primary branches, number of secondary branches, number of tertiary branches, girth of the branches, stem height, bush diameter, inter canopy distance and total number of bushes in the plot of 5m x 5m. After collecting the samples of the tea bush from the field, they were brought to the laboratory for the determination of weight of each sample. The samples were hot oven dried at 80°C and then weighed. The weight was recorded until a constant weight was observed. The weight was measured in grams. The weight thus recorded gives the bush sample biomass readily. The overall biomass of the bush was reconstructed by the field inventory data collected. The consideration given was that all the primary branches of tea bush were alike; and the similar consideration was made for all the secondary branches and all the tertiary branches too. The sum of the weights of all the branches thus gives the overall biomass of the tea bush in a sector. In this fashion, the biomass was calculated sector wise for all the sectors.

6.4. Retrieval of the Model Parameters:

The model parameter retrieval is implemented as per follows:

- a) The water cloud model parameters are retrieved one by one starting from the image values. The total power values, the backscattered values from the surface and the canopy are retrieved from the image. These values pertain to the σ_{tot}° , σ_{sur}° , and the σ_{vol}° . The ground collected data is divided into two parts: training and validation. The inverted water cloud model is utilized to estimate the values of biomass .
- b) From the training data, least square approximation method is used to estimate the value of the two way attenuation coefficient (ψ); regression analysis between the backscatter measured and the volume. The least square approximation calculates a straight line that best fits the data. The least square method considers that the best fit curve for a given curve has the minimum sum of the deviations, squared from the data set given. This fitting of the curve process, fits equations of approximating curves to the field data collected (i.e. the raw data). However, this curve is not unique for the dataset and thus a particular curve which has a minimum deviation

from all the dataset points is chosen. The complete process is an approximation of finding the minimum deviation curve and hence the name, Least Square Approximation [54]. Finally, the value of ψ is estimated and the constant. This value of ψ is retained for validation of the model. For proving the best fit of the retrieved model parameters, further validation was carried out on the validation data.

From the back-scatter values, the parameters of the water cloud model were extracted from the SAR image. The parameters are the surface scattering (σ_{sur}°) and the volume scattering (σ_{vol}°). The backscattered image is decomposed to retrieve the surface scattering and the volume scattering images. Fig. 6.1 shows the Sarusarai tea estate as in the SAR backscatter image. The values thus obtained were divided into two parts: the data for training the model, and the data for the validation of the model. The training data is utilized to estimate the value of the attenuation coefficient (ψ). The ψ value retrieved from the water cloud model with the help of least squares approximation is 0.016 kg/m^3 . This value of ψ thus obtained is utilized along with the σ_{sur}° and σ_{vol}° values of the validation data, in the water cloud model, to estimate the biomass of the samples for the validation data.

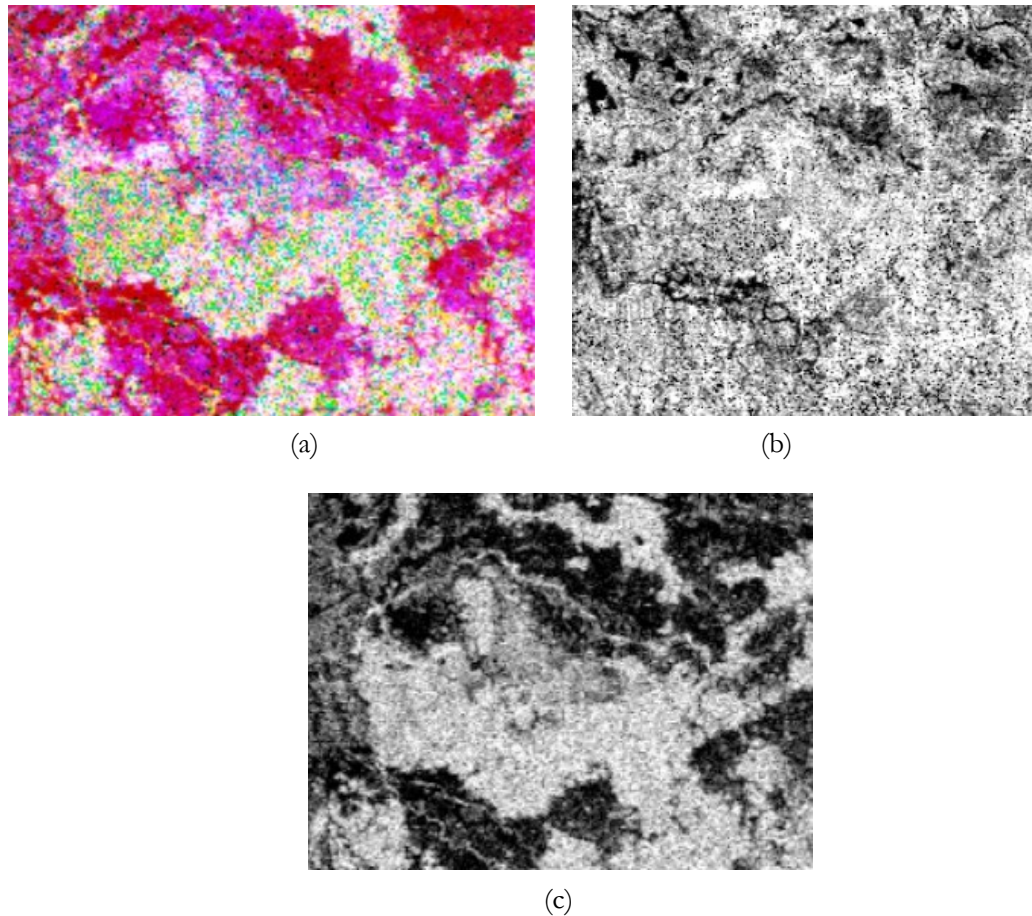


Fig.6.1:The Sarusarai Tea Estate (The Pauli RGB generated(a),surface scattering image(b), volume scattering image(c)).

The relation between the values of the backscatter and the volume, by the water cloud model is as shown in the figure (6.2).

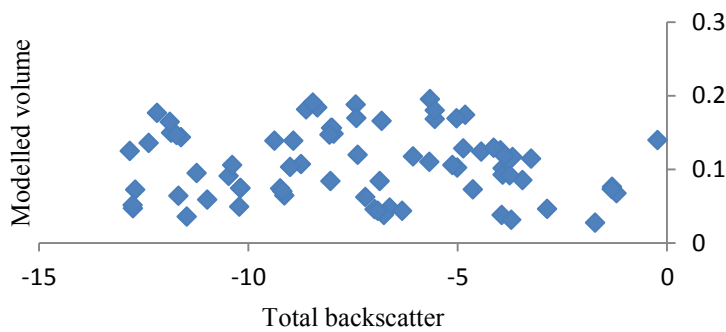


Fig. 6.2: Relation between the total backscatter (dB) and the modelled volume (m^3)

Fig. 6.2 indicates that for a certain range of values of the volume of tea bushes in a sector, the backscatter value remains unchanged (for example, when volume ranges from 0.1 to 0.2 m^3 the backscatter value is -5.0 dB). Also, this is observed for the overall volume distribution, see Fig. 6.2. This could be due to the reason that during pruning, the height of the bushes is restricted to a certain limit and twigs are also cut, and hence the backscatter amount becomes more or less same for the bushes. The canopy might increase in terms of width or diameter but this does not affect the backscatter value beyond a range. Fig. 6.2 indicates that the water cloud model is capable of giving the tea-bush volume in terms of the backscattered value, but for certain effective physical state of the bushes (that is, the combination of all types of stems, branches and twigs produces the combined surface and volume scattering values that have small range of change). Fig. 6.2 shows that the tea-bushes of different sectors are having similar volumes, but they show different backscatter values.

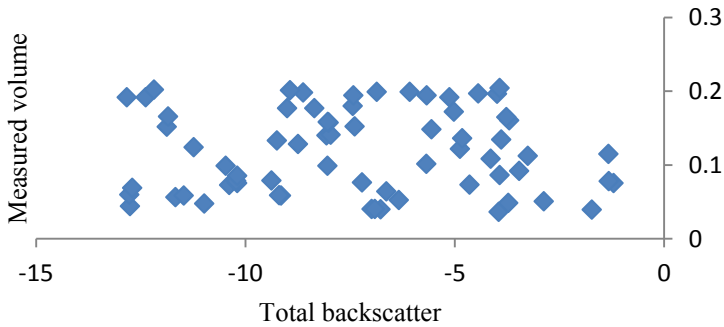


Fig. 6.3: Relation between the total backscatter (dB) and the measured volume (m^3) per plot.

Similarly, the Fig. 6.3 shows the plot between the measured volumes of the bushes per plot (5m x 5m) and the total back-scattered values. Again, as in the case of modelled volume estimation (Fig. 6.2), the measured volumes of the tea-bushes display a range for the same back-scattered value (Fig. 6.3). Like Fig. 6.2, the Fig. 6.3 also shows that the tea-bushes of different sectors are having similar volumes, and hence they show similar backscatter values too. This suggests that the volume of the tea bushes is identical and hence in many cases have similar backscatter values. Of course, there is no denying fact that the component scattering has something to play

a role in case of estimating the tea-bush volumes. This is because in those places where the surface scattering is low, the volume scattering is high (from the canopy), thus the overall backscattered energy remains within the shown range. For the area under study, the backscatter remains more-or-less within a certain range and the volume is distributed within this range.

6.5. Distribution of the tea bushes in the study area:

The category wise distribution of the tea bushes throughout the study area (tea estate) has been depicted in the figure (6.4).

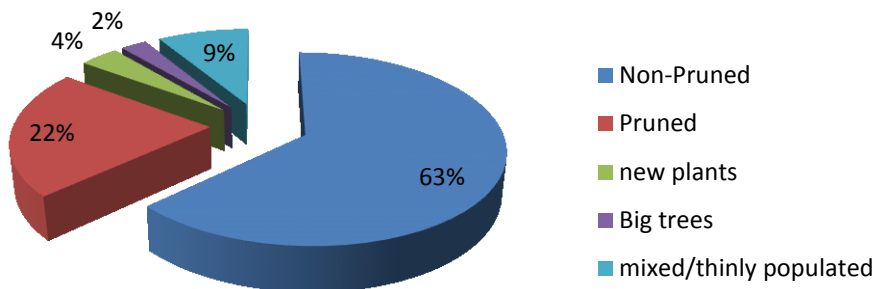


Fig. 6.4: Distribution of the tea bushes in the study area pertaining to their type.

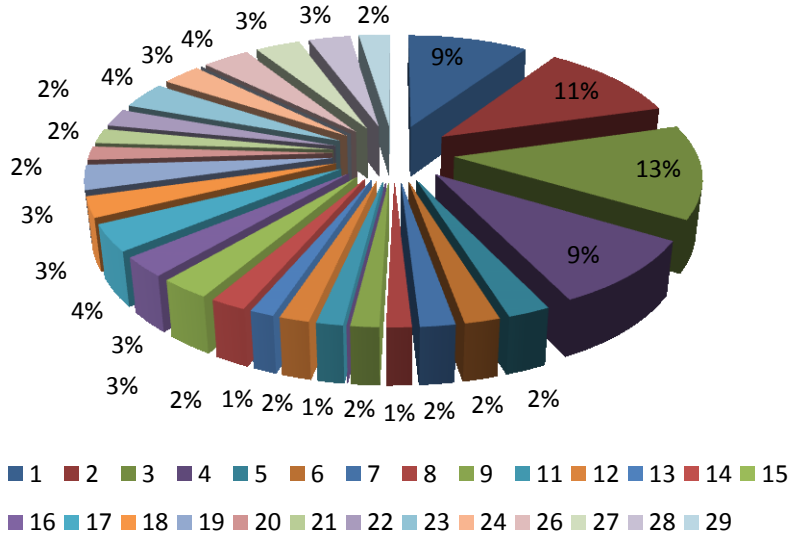


Fig. 6.5: Percent area wise distribution of the sectors. The legend denotes the sector number.

The above figure (6.5) represents the area wise distribution of each sector in the tea garden in percentage. The areas considered are in hectares. The largest sector being the sector 3 (area: 19.59 ha.) and the smallest sector 13 (area: 2.03 ha.). The previous figure shows that most of the bushes were non-pruned at the time of field survey.

6.6. Retrieval of Stem Volume using scattering:

The Fig. 6.6 shows the relation between the stem volume and the modelled biomass of the tea bushes of the tea estate. The stem volume is higher within the range of 0.001m^3 to 0.002m^3 approximately.

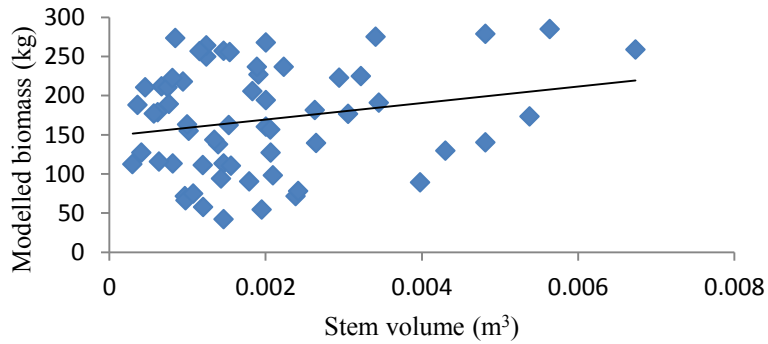


Fig. 6.6: Relation between the stem volume (m^3) and the modelled biomass(kg/m^2).

The relation of the stem volume with the biomass suggests that the biomass is more-or-less constant for a particular range of stem volume (Fig. 6.6). suppose if the stem volume is considered as 0.002m^3 , the biomass ranges from 54 kg/m^2 to 267 kg/m^2 roughly. This clearly indicates that the biomass is also dependant upon the age of the bushes, because the biomass would vary only if the number of branches increase (i.e. the canopy size increases) for stem volume remaining nearby constant. However, there is variation in the biomass with respect to the stem volume, i.e. increases which also indicates that biomass would definitely increase with the increase in the volume of the stem. Still, in the present case it seems that the SAR data/the model is not very efficient to bring this relation out effectively. Thus the stem of the bushes are nearly at similar height and due to the aging, the branches increase which result in increase in the biomass. Thus, the biomass has no direct relation with the stem volume of the tea bushes.

6.7. Relation between Biomass and the area of sector:

The details of the area of the sector and the biomass is depicted as in the table 6.1. The table indicates more than one aspect. Firstly, the biomass does not increase continuously with the area of the sector. Secondly, there is lots of variation in the area as well as the biomass indicating that a bigger area may have less biomass as compared to a smaller area which may have higher level of biomass. There are reasons. If the number of bushes are more in a small area, the biomass is higher, provided they are mature bushes. If the bushes are young the volume decreases and hence low biomass will be recorded. Further, a large area, if has sparsely populated bushes, will result in low biomass even if the bushes are mature (grown up). The biomass amount depends on some important factors like the age of the plants in the sector, the number of bushes in the sector and the canopy size.. Also, in some case if the bushes are pruned and the area is large, the biomass will be less. Even the smaller areas with unpruned bushes will give more biomass.

Table 6.1: Biomass and area of the sectors

Sector number	Biomass (kg/m ²)	Area of Sector (m ²)
1	186.8626569	143000
2	144.6467225	168100
3	332.2984791	195900
4	111.30981	140200
5	2.938512747	35700
6	98.356358	29600
7	114.8653379	29200
8	90.91459167	20700
9	81.73949467	23600
11	80.64428325	22300
12	299.0800221	25000
13	110.4528023	20300
14	86.54203053	30300
15	199.4816567	42500
16	174.8022046	41700
17	257.149202	56100

18	234.4703513	43200
19	165.8236905	51900
20	101.776224	28500
21	111.9134304	31400
22	243.8992221	37100
23	212.7198787	55600
24	107.6225732	46200
26	299.0629136	55400
27	474.9288184	52500
28	239.9048391	49000
29	211.6038674	36400

6.8. Relation between Volume and Height of the bush:

A relation was sought between the height of the tea-bushes of sectors and the volume of the tea-bush, which is shown in Fig. 6.7. The plot shows that as the height increases from 0.5 m to 1.3 m, the volume of the tea-bush gently increases (Fig. 6.7). It is observed that when the height of the tea-bushes reaches a limiting height, the volume of certain sectors keep on increasing. This could be due to the reason that as the bush is ageing, the number of branches increase along with the increase in the diameter of the branches/stems, and thus the volume of the tea-bush increases. The height of the bushes in the tea estate does not fluctuate so much; whereas, the volume of the bushes increases slowly. Most of the bushes are within the height range of 0.4 m to 1.3 m. Also, the stem volume of the bushes varies considerably for deviations in the height of the bush. This is basically due to the fact that the bushes are pruned after a certain height and maintained up to that level. Thus, pruning results in the check of the height of the bush but the girth of the bush increases slowly with age.

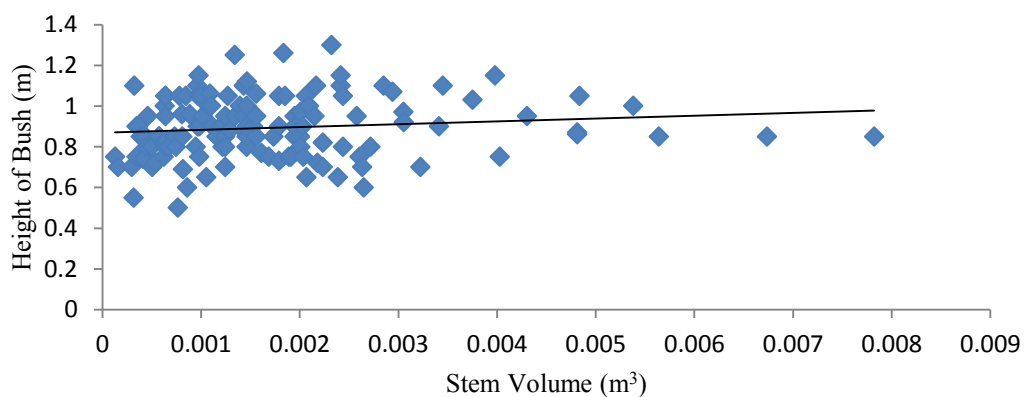


Fig. 6.7: relation between the stem volume (m^3) and the height of the bush(m)

6.9. Relation between the modelled volume and the Ground measured volume:

The scatter plot between the modelled volume (m^3) and the ground measured volume (m^3) is shown in Fig. 6.8. The good fit straight line through these scatter points indicates that the correlation between the modelled volume and the ground measured volume is quite acceptable. The term acceptable deals with the penetration capability and the condition of saturation. The relation between the modelled volume and the ground measured stem volume also depends on the status of the bush, whether it is pruned or not pruned. The volume thus calculated from the model (also refer to equation 6.5) shows the optimal correlation with the field values. On the ground the area under study has mixed features such as tea-bushes, open ground, the large canopy gaps and even the inter bush gaps which are highly non-uniform. Every sector has different kind of bushes and gaps. Some are pruned, others are non-pruned. This leads to a large deviation in the resultant values. For getting the proper value of the tea-bush volumes, the estimation is to be made on individual sectors. And, accordingly, after applying the model on individual sectors, the results thus obtained show even better correlation values (Fig. 6.9a and Fig. 6.9b). Fig. 6.9a gives the plot of the measured volume versus the model estimated volume for non-pruned sectors; whereas, the Fig. 6.9b shows the plot between the measured tea-bush volume and the modelled tea-bush volume for pruned sectors. Since the SAR data used in the present study is of the month of April and the field data has been collected in December. Therefore, the field inventory data and the information captured on the image are expected to be corroborative, and which may be assumed as the favourable condition for the model to provide relatively accurate values of the tea-bush volumes for the pruned sectors only. Fig. 6.9b justifies this statement as the coefficient of determination ($R^2 = 0.8431$) is found to be quite high for pruned sectors. In contrary, the Fig. 6.9a shows that the condition and the physical state of the bushes were quite different during the image capture than the field survey period for the un-pruned sectors, that is why, it yields moderate value of the correlation ($R^2 = 0.468$). Thus, for SAR polarimetric analysis, it is equally important to get the synchronised image and in situ data.

The retrieval of the volume is done using the PALSAR backscatter data. By inverting the semi empirical model, i.e. water cloud model, values for the volume is retrieved. This process is applied on the backscattered values for every plot. The backscattered values have been obtained from the SAR image (section 6.4). For every such plot, the volume measurements are retrieved. After inverting, the volume can be retrieved from the following equation:

$$V_i = -\frac{1}{\psi} \left[\ln \left(\frac{\sigma_{tot,i}^\circ - \sigma_{vol}^\circ}{\sigma_{sur}^\circ - \sigma_{vol}^\circ} \right) \right] \quad 6.5$$

where: V_i = stem volume for each plot; and
 ψ = two way transmissivity.

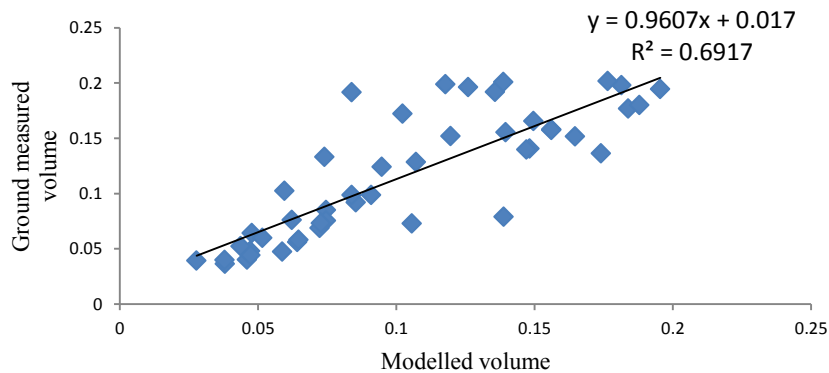
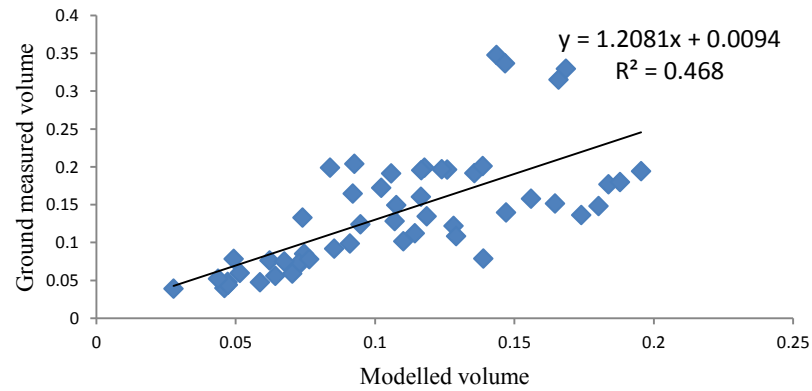
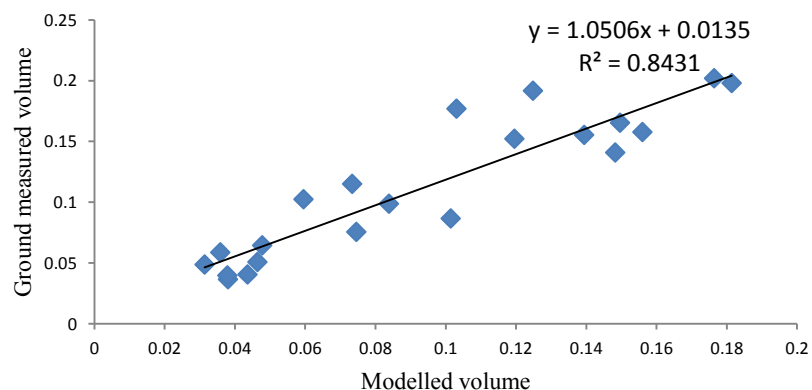


Fig. 6.8: Relation between Ground measured volume (m^3) and modelled volume (m^3)



(a)



(b)

Fig. 6.9: Relation between the modelled volume (m^3) and the ground measured volume (m^3),
(a) the non-pruned bushes, (b) the pruned bushes.

6.10. Above ground biomass retrieval using the backscatter:

The above ground biomass has been retrieved by the technique similar to that followed in the volume retrieval. The water cloud model equation used for the retrieval is as follows:

$$\sum_{i=1}^n \sigma_{m,i}^{\circ} = \sum_{i=1}^n [\sigma_{sur,i}^{\circ} e^{-\psi_i B_i} - \sigma_{vol,i}^{\circ} (1 - e^{-\psi_i B_i})] \quad 6.6$$

where; $\sigma_{m,i}^{\circ}$ = measured backscattered value,

$\sigma_{sur,i}^{\circ}$ = backscattered value from the surface,

$\sigma_{vol,i}^{\circ}$ = backscattered value from the canopy.

B_i = biomass of the i^{th} plot

The above ground biomass is retrieved from the following equation obtained from the above equation:

$$B_i = -\frac{1}{\psi} \left(\ln \left(\frac{\sigma_{mod,i}^{\circ} - \sigma_{vol}^{\circ}}{\sigma_{sur}^{\circ} - \sigma_{vol}^{\circ}} \right) \right) \quad 6.7$$

The biomass retrieved is from a single time period data. After substituting the retrieved values of the water cloud model in the above equation (6.7), the tea bush above ground biomass is retrieved for every plot of the tea garden. The following figure 6.10 shows the relation between the ground measured biomass and the modelled biomass:

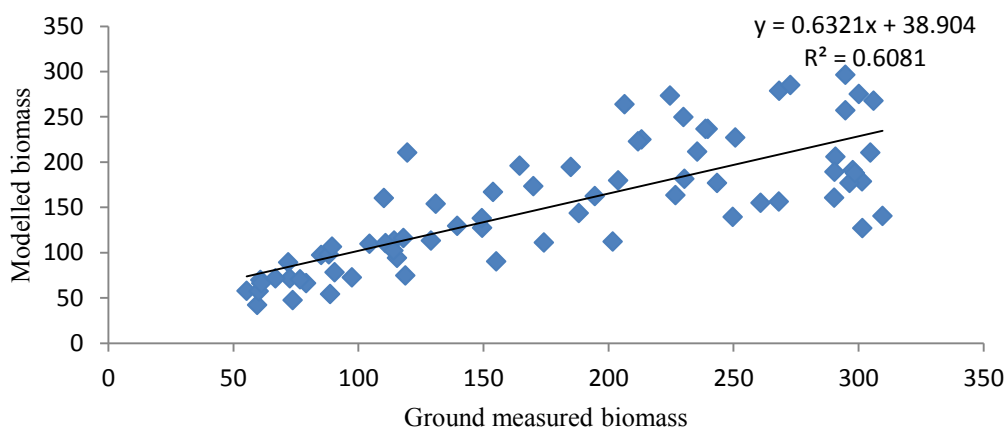


Fig. 6.10: Relation between ground measured biomass (kg/m^2) (X-axis) and the modelled biomass (kg/m^2) (Y-axis).

Further, The Fig. 6.10 depicts the capability of the water cloud model to retrieve biomass of the tea bushes from the PALSAR backscattered image. The model is assisted with the measurements which have been carried out in the tea estate. The relation shows that there is a positive correlation of more than 60% between modelled and estimated biomass of tea-bushes

of different sectors. Thus, the Fig. 6.10 shows that the biomass retrieved from the water cloud model has a better correlation with the ground measured in-situ data; and it is found that the correlation between the modelled biomass and the ground measured biomass is about 0.61. However, the actual field of tea-estate comprises of bushes broadly of two kinds, i.e. pruned and non-pruned. The above ground biomass thus retrieved is a combination of both kinds of bushes. Hence an attempt has been made to evaluate the biomass of the pruned and the non-pruned tea-bushes separately. The Fig. 6.11a and Fig. 6.11b show the relation between the biomass as that retrieved from the model and the in-situ ground measured biomass for un-pruned and pruned bushes, respectively.

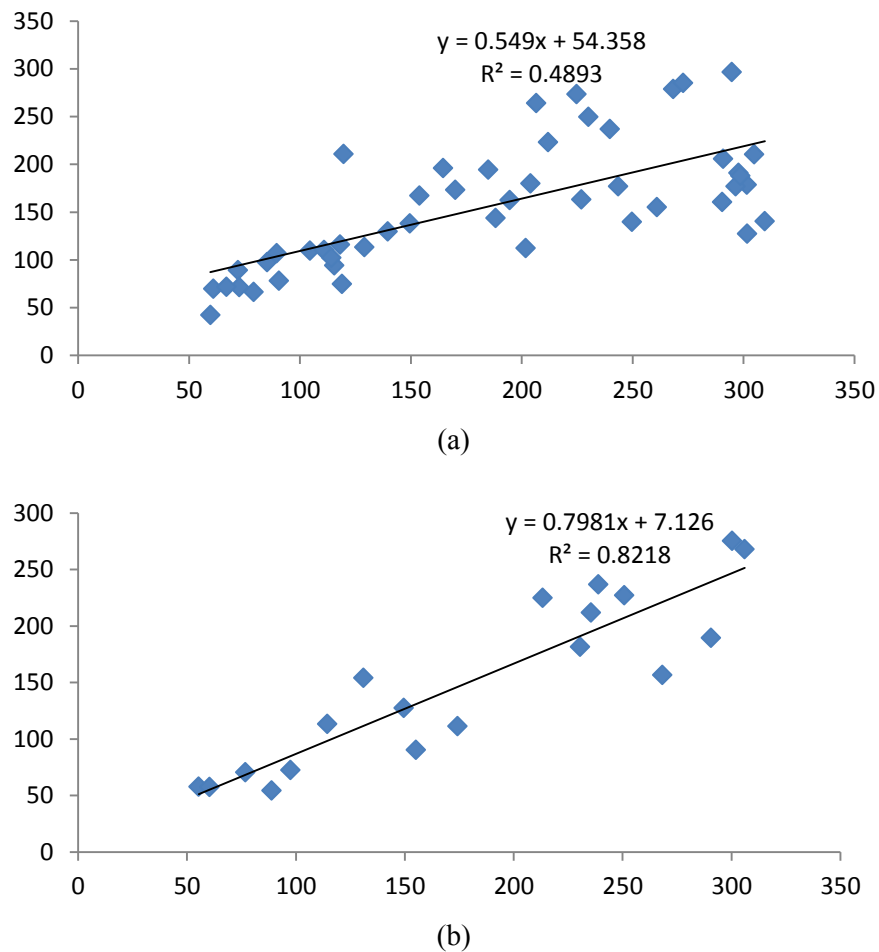


Fig. 6.11: Relation between ground measured biomass (kg/m^2) (X-axis) and the modelled biomass(kg/m^2) (Y-axis). The non-pruned bushes(a), and the pruned bushes (b).

The Fig. 6.10 and Figs. 6.11(a & b) display that the biomass obtained from the model has relatively better values when implemented on well distributed bushes. Often some plots having low biomass, show higher value when the value is retrieved from the water cloud model as compared to the in situ data. This kind of error often occurs due to the saturation and the noise in the backscatter values. However, the capability of the model is found to be highly promising for the homogenous distribution of tea-bushes in sectors, such is the case for the pruned bushes (see Fig. 6.11b).

6.11. Relation of volume and biomass:

In Fig. 6.12, a relation between the measured volume (m^3) and the modelled biomass (kg) has been plotted to extract definitive information regarding above ground biomass of tea plantations. A best fit straight line has been drawn through the scatter points to demonstrate that when the measured volume corresponds to this line will provide a definite tea biomass of those sectors which have tea-bushes of the average age group lying close to this line. The points which lie above this line, although with large volume, have the tea-bushes of the sectors of relatively of younger age group and produces less tea biomass. Because the young tea-bush has more moisture in stems, branches, twigs and leaves, there will be effective backscatter. The points which lie below this line expectedly must belong to much older age group with relatively dense stems, branches, twigs and leaves bearing less moisture part and respond for more modelled tea biomass (Fig. 6.12). This suggests that older the bushes are, higher the density of the wood and hence more the tea biomass. Thus, conclusively, it may be stated that the decreased water content of the tea-bush is always associated with older tea plantations in the estate having less wood volume which provides higher above ground biomass .

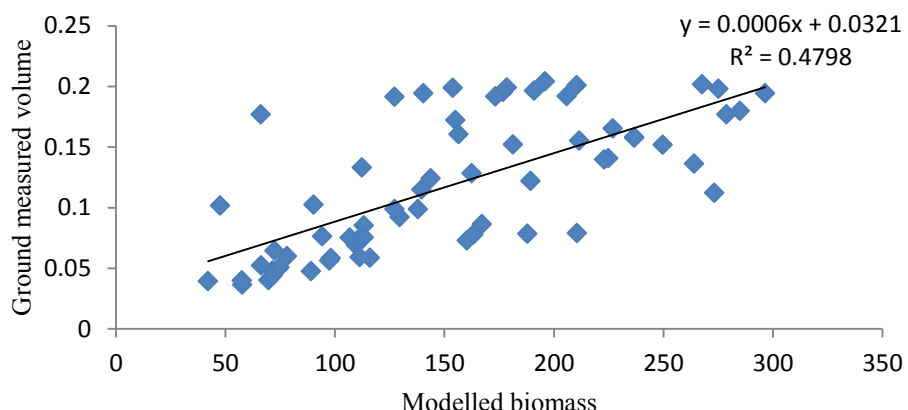


Fig. 6.12: Relation between the modelled biomass (kg/m^2) and the ground measured volume (m^3)

6.11.1. Relation between volume scattering and biomass:

The relation between the volume scattering and the modelled biomass has been shown in the Fig. 6.13. Fig. 6.13 indicates that for a certain range of values of the biomass of tea bushes in a sector, the volume backscatter value remains unchanged, e.g. when the tea biomass ranges from 70 to 280 kg the backscatter value is -5.0 dB. Also, this is observed for the overall biomass distribution, see Fig. 6.13. This is mainly due to the fact that, during pruning, the height of the bushes is restricted to a certain limit, and hence the backscatter amount becomes more or less same for the bushes. The plot also indicates that the water cloud model is quite adequately giving the tea biomass in terms of the volume backscattered value. If the Fig. 6.13 is compared with Fig. 6.2 for scattering, it will be obvious that the volume scattering is a dominant component in overall back-scattered value in tea estates. However, there are differences, particularly, for the area under study; the same volume backscatter is displayed for a range of values of tea biomass. And, in the entire area, the volume scattering occurs within a range from -0.5 to -10.5 dB and the biomass value is limited within 40 to 300 kg. Thus the

changes in the volume backscatter is not very abrupt which implies that the volume and thus the biomass of the bushes are very sensitive to the volumetric scattering.

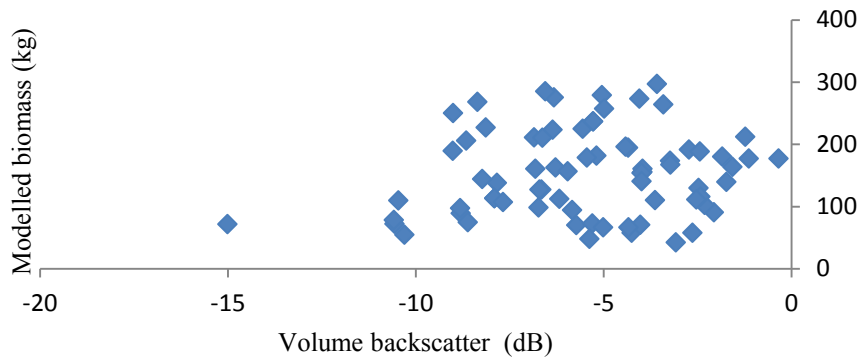


Fig. 6.13: Relation between the modelled biomass (kg/m^2) and the backscattered volume (dB)

6.12. Relation between bush canopy and biomass:

A scatter plot relating the tea-bush canopy and the modeled tea biomass is depicted in the Fig. 6.14. A good fit line is drawn through scatter points only to see the nature of the average age it would represent and the behavior between these two parameters. If this trend line corresponds to the average age (40-50 years), the increase in bush canopy produces less biomass; which clearly indicates that the tea-bushes were not pruned sufficiently in time, resulted in excessive growth of twigs and leaves. The points which lie above and below this line only correspond to higher and lower than the average age group, respectively. Therefore, for the same canopy size of the tea-bush, the tea biomass increases with age (Fig. 6.14). Thus, due to periodic pruning and constant maintenance, the bush diameter is limited to about 2.5 m and the biomass varies within this range of the diameter.

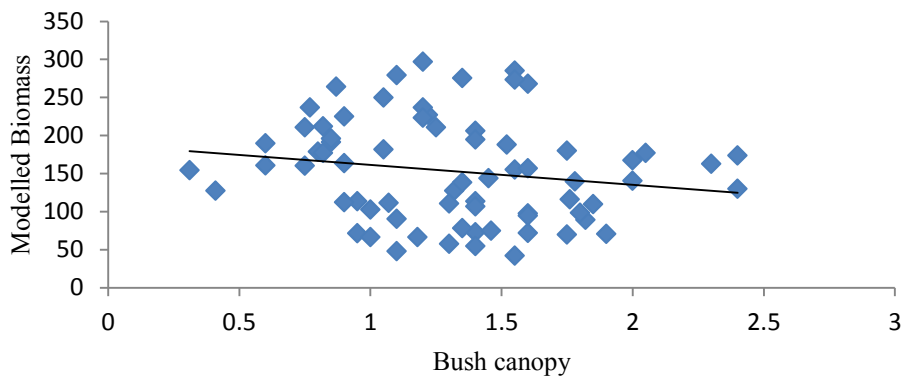


Fig. 6.14: Relation between the bush canopy diameter (m) and the modelled biomass (kg/m^2)

6.13. Relation between total backscatter and the modelled backscatter:

The relation between the total bacscattered value and the modelled backscattered value is as shown in the Fig. 6.15. The values denote the energy recorded that is scattered back from the bushes. There is a wide range of variation in the modelled back-scattered. The plot shows that the range of total back-scatter value is from -0.07 to -2.6 dB; and the range of modelled back-scatter value is from -3.8 to -12.8 dB.

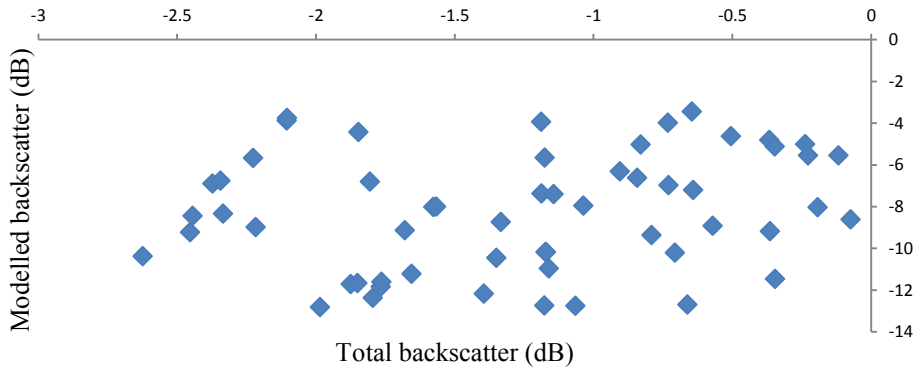


Fig. 6.15: Relation between the total backscatter (dB) and the modelled backscatter (dB).

6.14. Relation between the backscattered component values:

The values of the surface scattering and the volume scattering for the tea estate as deduced from SAR image are plotted in Fig. 6.16 which display the typical nature of scattering mechanism for dense bushes. Fig. 6.16 shows that the two curves are quite distinct in nature with negative values. The two curves signify the importance of scattering mechanism in the case of study of bush biomass through microwave remote sensing. It is obvious from Fig. 6.16 that the numeric values of surface scattering are more than the numeric values of the volume scattering. These differences in the scattering values denote that when the scattering from the canopy takes place, the surface scattering is low (here low negative deflection), which is

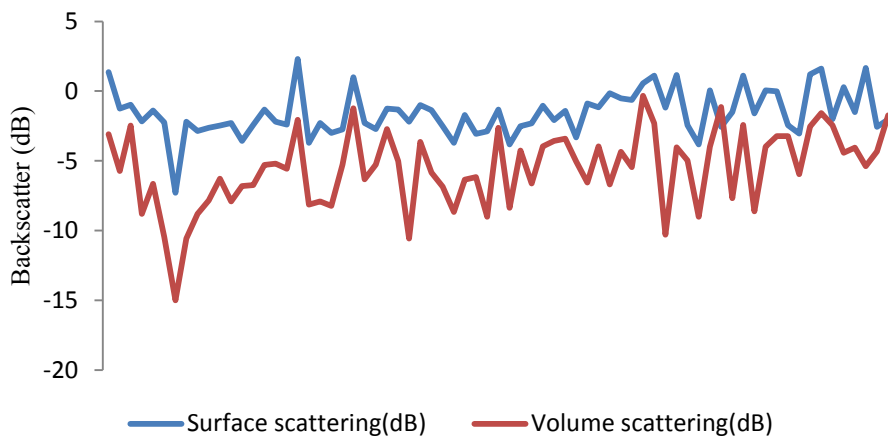


Fig. 6.16: Relation between the volume scattering (dB) and the surface scattering (dB).

obvious as discussed in the section 6.11.1. In the absence of canopy structure, the incident microwave energy directly interacts with the ground and the surface backscattered value becomes higher. It is observed that, for tea-bushes in sectors, the volume scattering is always the dominant component, and it needs more and more future studies to establish its concreteness.

6.15. The model evaluation:

The performance of the model is evaluated as per the commonly considered statistical parameters that are; coefficient of determination (R^2) and the root mean square error (RMSE). This is necessary in order to describe the results of the estimated bush biomass. The ground truth measurements are reliable at plot level. The figures show that the coefficient of determination is of acceptable accuracy. The root mean square error, for the plots for retrieved biomass is also of acceptable level. The RMSE has been calculated as follows:

$$RMSE = \sqrt{\frac{1}{N} \sum_{i=1}^N (B_i^{model} - B_i^{measured})^2} \quad 6.8$$

where, B_i^{model} is the modeled biomass per plot, $B_i^{measured}$ is the measured biomass per plot and N is the number of plots from the *in-situ* data.

After using the equation 6.8, the RMSE for the estimated biomass has been obtained as 59.33. The Fig. 6.10 or Fig. 6.11(a&b) shows the relation between the ground measured biomass and the modeled biomass. The coefficient of determination is appreciable, which is 0.61. The average absolute accuracy for the estimated biomass is calculated as [62]:

$$\varsigma_m = 1 - \frac{1}{N} \sum_{i=1}^N \frac{|B_i - A_i|}{A_i} \quad 6.9$$

where, ς_m = Average accuracy

B_i = estimated modeled biomass per plot

A_i = ground estimated biomass per plot

N = number of plots

Thus the average accuracy is defined as $\varsigma_m \times 100\%$. The average accuracy estimated for the above ground biomass turns out to be approximately 79% which is acceptable. Thus the water cloud model shows positive capability of estimating the above ground biomass of the tea bushes from the SAR data.

6.16. Discussion:

As the researches are still continuing with the conventional remote sensing techniques for estimating the biomass of vegetation including the tea estate; the determination is not so accurate, particularly, for low height vegetation with dense canopy structure such as tea-bushes. A continuous effort is being made to replace the traditional methods of biomass estimation with the polarimetric SAR technique. Especially, this is because of the SAR having higher penetration capability. Encouraged by this fact, the present study, concerning tea-bush biomass assessment through microwave remote sensing has emerged. The biomass estimation in the present scenario still remains a challenging task in inaccessible areas and low height vegetation, such as tea bushes.

The objective of the present study is to estimate the tea biomass through polarimetric decomposition and modelling with WCM model. The modelling comprises of two steps procedure: training and validation. To effect this, it is the first and foremost importance to collect in situ field data of the area under study, i.e. the Sarusarai Tea Estate, Toklai in Assam. The study area which covers the STE is bounded within (Lat: 26.29° - 26.95° N and Long: 94.03° - 94.47° E) was visited for the collection of ground truth and tea inventory. The study area is divided into 38 sectors which comprises 160 sample plots with each plot is of the size 5 m x 5 m. The training of the model and retrieval of model parameters has already been described in sections 6.2 and 6.4.

An iterative process has been adopted for training the model. This is basically done to prevent from the errors that might be present because of the spread of the backscatter data. Another cause is the low sensitivity towards the volume. This is chiefly because of the fact that the bushes are of low height and in some cases the canopy is highly dense. However, as soon as the parameters of the water cloud model are retrieved, the bush biomass assessment becomes possible. This is basically done through the inversion process of the water cloud model (section 6.9). The modelled biomass are well correlated with the ground measured biomass. This relation is often affected by the distribution of the bushes in the study area. As homogenous the distribution of the bushes are, the biomass retrieved by the model proves to be in good agreement with the field data. This is again because of the reason that the heterogeneous distribution will have unequal canopy gaps and the areas will also contain the garden roads and open grounds, i.e. the non-vegetation patches. Also the unequal interval of the bushes decrease the overall efficiency of biomass retrieval by the model. The results suggest that the biomass retrieval is best when the sectors are homogenous and the stem volume is high. Thus the root mean square error is quite low. However the dense canopy often becomes a limitation. Another limitation was the difference between the dates of the captured data (image) and the field survey. In the absence of purely synchronized data, some differences between the modelled volume retrieved from the back-scattered values and the field measured volume have been observed, see Fig. 6.8 with $R^2 = 0.6917$ for overall tea estate. The modelling results show that there is satisfactory correlations between the modelled and the measured biomass for overall tea estate, see Fig. 6.10 with $R^2 = 0.6081$. After classifying the data for unpruned and pruned sectors, and when modelled it separately for unpruned and pruned bushes, the results were very satisfactory. For example, the plots of modelled volume versus measured volume (in situ data) yield results: (i) Fig. 6.9a, for unpruned tea-bushes with $R^2 = 0.468$; and (ii) Fig. 6.9b, for

pruned tea-bushes with $R^2 = 0.8431$. Similarly, the plots of modelled biomass versus measured biomass yield results which are more appropriate and correlated with the ground data: (i) Fig. 6.11a, for unpruned tea-bushes with $R^2 = 0.4893$; and (ii) Fig. 6.11b, for pruned tea-bushes with $R^2 = 0.8218$. Thus, the performance of the semi-empirical model is found to be satisfactory in respect of estimation of biomass of tea-bushes of tea-estate when applied on the appropriately classified data, to set data homogenised as per requirement of the model .

The modelling results could be improved further provided training data is free from locational/ positional errors. The main cause of locational/ positional errors is that the GPS receiver used to record the plot locations were not highly accurate for the purpose of locating the tea bushes. The GPS receiver used had a positional resolution of 5 m only. Every plot considered was of size 5m x 5m in the present study. There could be misplacement in image pixels due to SAR geocoding technique. The plot areas are surrounded by roads and often with open empty grounds. A little shift or error in the location values will result in change in pixel value. Therefore, any kind of mismatching in the positioning of in situ data with GPS and geocoding of the image pixels will result in error. Also, there is a lag of about six months between the actual time of field survey and the time of capture of the image of tea bush biomass which is used for the analysis using the polarimetric decomposition and the semi-empirical modelling techniques. That is why the assessment of the model performance for the estimation of the ‘above ground biomass’ sometimes becomes otherwise at par. However, the stem volume has been retrieved by the Water Cloud Model (WCM) with the optimised parameters using the SAR backscattered images. The coefficient of determination i.e. the R^2 value is about 0.69 to 0.7. The section 6.10 shows the potentiality of the Water Cloud Model (WCM) in tea bush above ground biomass estimation. The parameters for the model were estimated for biomass retrieval, and the root mean square error is obtained is about 20.

Further, the plot between the height of the bushes and the stem volume was also sought and it shows (Fig. 6.7) that the relation is more or less constant but there is a level beyond which the values do not change. The plot shows that as the height increases from 0.5 m to 1.3 m, the volume of the tea-bush gently increases. It is observed that when the height of the tea-bushes reaches a limiting height, the volume of certain sectors keep on increasing. This could be due to the reason that as the bush is ageing, the number of branches increase along with the increase in the diameter of the branches/stems, and thus the volume of the tea-bush increases. This is basically due to the fact that the bushes are pruned after a certain height and maintained up to that level. Thus, pruning results in the check of the height of the bush but the girth of the bush increases slowly with age. There were very few tea trees which were more than 6 feet in height at the time of field survey. These high trees were kept so, to protect some mother plants in order to retrieve twigs for producing new plants. This process in itself is called *Grafting*. When the twigs grow to certain height, they are transplanted into the field in order to grow completely to develop as an independent tea bush. The new plants, have narrow twig like stem with no secondary branches or tertiary branches and thus have very low biomass. The height of the bushes range from 0.5 m to 2.5 m. the bushes are of the height variation of 0.5 m to 1.1 m. The tea trees have much higher height of about 2 m to 2.5 m and even a little more. Also, the dense shrubs in between the tea bushes in some sectors were a cause of higher backscatter value in some pixels, resulting in higher values of biomass.

7. CONCLUSION

7.1. General:

Tea is primarily the most popular and important beverage in India, and in other parts of the world. India is among the major tea producer and exporter countries of the world. A lot of emphasis is given for the economic production of tea, which is again related to the proper cultivation of tea giving high yield. A review of literature shows that, although, lots of research and studies has been carried out to estimate the biomass of the forests but a very few studies focused on the estimation of biomass of tea bushes. The present study is an attempt to overcome this limitation and provides a possible solution to this effect. In this regard, the previous studies reveal that the capability of optical data to resolve this kind of problem to estimate the ‘above ground biomass’ is limited, particularly, because of low penetration power of electromagnetic radiation in the optical range; whereas, the microwave SAR data scores over optical data in this respect. And, the SAR data has been used extensively to estimate the biomass of trees in forests. The resolution and accuracy of estimating the biomass of forest regions is found to be quite high. Thus, in the present study, the emphasis has principally been laid to extract the ‘above ground biomass’ of tea bushes in the tea estate of the State of Assam, India. The result generated from this study reveals that the SAR data can be used to estimate the above ground biomass of tea bushes. The error is low and hence the result obtained is appreciable. The field data has been collected for the study area which covers the Sarusarai tea estate is bounded within Latitude: 26.29° - 26.95° N and Longitude: 94.03° - 94.47° E.

Therefore, the prime objective of this study was to retrieve the ‘above ground biomass’ of tea bushes, by the polarimetric decomposition technique utilizing semi-empirical model. A model based approach has been used for this study to retrieve the above ground biomass, and the volume of tea bushes. The conceptual model that has been followed is the water cloud model, which was integrated with the PALSAR information. The training of the model was based on 80 tea garden samples (one plot represents one sample) measured on the ground. The measurements comprised mainly the volume, the height and the distribution of the tea bushes of the study area (tea estate). The training process comprises the determination of two way attenuation of the incident energy, and obtaining the backscattered energy information which were then used to test/ validate the so generated trained model to obtain the biomass. For validation, the model was applied on 80 plots of the tea garden. The model result shows the relationship between the backscattered values and the volumes which yields the biomass of tea bushes. The relation thus obtained shows that as the magnitude of the backscatter increases, the increase in the volume is limited only to a particular range. This implies that when the bushes are fully matured/ developed, the stem volume does not increase after a level when the similar backscatter values are reached in the neighbourhood.

For the retrieval of the stem volume with the water cloud model, the value of the coefficient of determination (R^2) is found to be about 0.61, and the root mean square value is found as approximately 59.33, which is quite appreciable for the present case. This implies that the performance of the model is good and is capable of retrieving the ‘above ground biomass’ of tea bushes from the SAR image. However, there are some constraints to this retrieval. Firstly, in nature, always there is the stratum wise distribution of the tea bushes which requires to be homogenised as the model is capable of handling only the homogenous patterns of distribution of bushes, and for getting the best results. Secondly, the types of bushes (old plantation, new plantation, pruned or unpruned) affect a lot on the estimation values. Further, it is found that there is a lag of about six months between the actual field survey and the time of capture of the image of tea bush biomass which is used for the analysis using the polarimetric decomposition and the semi-empirical modelling techniques. That is why the assessment of the model performance for the estimation of the ‘above ground biomass’ sometimes becomes otherwise at par. It is expected that if there is one-to-one correspondence between the time of field data collection and the transit time of satellite for SAR imageries, the model performance would be even better. Moreover, this is very important because the physical state of the bushes change (pruned or non-pruned). The tea bushes are pruned thrice a year. From the optical image it is quite evident that the bushes which are non-pruned get pruned after few months thus proving to be the main cause of getting differences in the results.

It is found that the model has the limited ability of retrieval of the ‘above ground biomass’ because of the reason that the bushes under consideration vary in physical structure and distribution. This makes the overall distribution of the bushes heterogeneous. The tea bushes were non-uniformly distributed and there was limited homogeneity in the type of bushes in a particular plot which the model demands. However, in the present study, the performance of the model under such circumstances, and keeping in view the constraints, is quite positive. The results showed that when the model is applied to the homogenous sectors with uniform distribution and with same age of bushes, the result is very satisfactory. Thus, it may be stated that the performance of the semi-empirical modelling with polarimetric decomposition of SAR data is found to be satisfactory in respect of estimation of volume and biomass of tea-bushes of Sarusarai tea-estate when applied on the appropriately classified data, as the classification satisfies the requirements of homogeneity.

This may be stated here that the values of ‘above ground biomass’ and volume of tea-bushes of Sarusarai tea estate of NE India as deduced from the SAR imagery using WCM model show good correlation with the ground measured data. Thus, the encouraging results out of the present study for tea-bushes indicate that there is definitely a high hope of estimating the above ground biomass and the bush parameters using the semi-empirical modelling approach utilizing polarimetric SAR data and the field measurements. *The model may further be tested on extensive in situ data for its future routine use in the estimation of biomass of tea estates.*

Henceforth, the results of the research questions are as follows:

Q1. How to utilize the scattering matrix elements for coherency matrix based decomposition to extract volume scattering and surface scattering information from polarimetric SAR data?

A1. The parameters are the scattering matrix components. To utilize the parameters for decomposition we first have to extract information from the scattering matrix thereby the generation and decomposition of the coherency matrix. To generate the coherency matrix which is the second order derivative of the scattering matrix, we first generate the target vector. First order derivative of scattering matrix is expressed by Pauli's basis representation. Pauli basis is defined by sum and difference of co-pol terms and twice the cross-pol term. The feature vector in Pauli basis is given by eqn. 2.6. Then, the next step includes the generation of the coherency matrix, T , formed by the Pauli target vector; eqn. 2.6. Thus the final coherency matrix looks like eqn. 2.6. Further, the coherency matrix is modeled on Bragg's law to extract information of ground scattering. The coherency matrix is represented in terms of surface scattering. It is defined as scattering from the interface between two dissimilar media, such as the atmosphere and the earth's surface. The surface scattering is the single bounce model, from slightly rough surface. The volume scattering results from particles present in a non-homogenous medium. Most of the natural surfaces are of an inhomogeneous composition. Under certain circumstances they are penetrated by the EM waves. Under normal conditions, scattering from natural terrain features consists of both surface and volume scattering. The dielectric discontinuities within the media result in the volume scattering.

The volume scattering is employed on a randomly oriented dipole. We further simplify by assuming thin cylindrical scatterers so that S_v equals one and S_h equals zero. Furthermore, we assume a uniform orientation distribution.

Q2. What is the relation between vegetation scattering and ground scattering for L-band fully polarimetric, tea plantation data?

A2. The main motivation in using the surface scattering and the volume scattering is to utilize the technique to retrieve the information of the vegetation cover and the ground cover (section 6.14).

Q3. What is the use of scattering mechanism and modelling to retrieve the water cloud model parameters?

A3. The concept of water cloud model describes the relationship between the tea bush backscatter and tea bush parameters. WCM assumes that vegetation acts like a water droplets filled homogenous medium. The scattering elements are the water droplets uniformly spread within the volume. All scatterers have the same properties thus, the total backscattered energy is the sum of energy scattered at each individual layer. In this case (as developed by freeman) the single scattering and the scattering by the tea bush canopy (volumetric) is to be considered. If the total backscatter is sigma nought (σ_{tot}^0) then the general water cloud model can be written as in eqn. 5.39.

- Q4. How to retrieve above ground biomass (AGB) with the help of the parameters?
- A4. The polarimetric decomposition based semi-empirical modelling development includes principles of WCM. The semi empirical model can be expressed as in terms of scattering matrix elements considering the surface and the volume scattering. The information has been utilized in the water cloud model. The contributed backscattering is weighed by the area fill factor. So, the semi empirical equation forms like: $\sigma_{tot}^o = (e^{-\psi_B})f_s + (1 - e^{-\psi_B})f_v$. Thus the complete eqn. is as shown in eqn. 5.42. For this, firstly, the data (samples) from the field is collected. In this case the total backscatter is considered as the sum of surface scattering and the volume scattering. The total backscatter i.e. the span image is generated. Few of the samples are used for the model training i.e. in the form of the attenuation coefficient (ψ). From the model the biomass will be estimated. Then for the rest of the samples of the collected data the biomass will be estimated from the water cloud model and it will be simultaneously compared with the ground collected biomass for verification and validation.
- Q5. What is the accuracy of the modelled AGB in comparison with the field measured AGB?
- A5. The accuracy of the modelled above ground biomass in comparison to the field measured biomass is quite appreciable. The root mean square error is approximately equal to 59.33. The coefficient of determination (R^2) is about 0.61. This means an error of approx..60 kg in biomass per plot (one plot is of size 25 m²). The R^2 value shows optimal correlation between the modelled values and the ground collected values. The model has limited ability of retrieval due to the reason that the bushes under consideration vary in physical structure and distribution, which makes the overall distribution of the bushes heterogeneous. The tea bushes were non-uniformly distributed and there was limited homogeneity in the type of bushes in a particular plot. Thus final conclusion drawn is that the semi-empirical model developed is able to predict the biomass of tea bushes from the SAR data which includes in-situ measurements.

7.2. Recommendations

Based on the earlier studies and the current study, the observation stays that the ground measured information is necessary for the estimation of above ground biomass. For the estimation of the biomass sole dependence on the remote sensing data is not possible. The semi-empirical model used in the current study estimates the above ground biomass of the bushes with the help of in-situ data. The capability of the model is average but this is dependant on few limiting factors like the type of the bushes and the distribution. Further, the biomass retrieved varies when compared with the in-situ data. This can be delimited by the use of multitemporal approach.

Another issue is that the model assumes the ground and the canopy backscatter values. The model does not consider the scattering from the combined backscatter of the ground and the bushes. This is another major reason for the differences in the modelled biomass and the *in-situ* biomass. Thus higher order of backscatter can be considered for further studies. Further, wide range of wavelength can be considered for the same for the water cloud model. The model can be tested with P-band data which is expected to give higher level of accuracy due to its characteristic feature of more penetration power. Multitemporal images can be used for better performance of the model.

LIST OF REFERENCES

8. REFERENCES:

- [1] T. Mette, K.P. Papathanassiou, I. Hajnsek, R. Zimmermann, "Forest biomass estimation using polarimetric SAR interferometry," *Geoscience and Remote Sensing Symposium, 2002. IGARSS '02. IEEE International* , vol.2, pp. 817- 819,2002
- [2] A. Freeman, "Fitting a two-component scattering model to polarimetric SAR data from forests," *IEEE Transactions on Geoscience and Remote Sensing*, vol. 45, NO. 8, pp. 2583-2592 , August 2007.
- [3] V. Nizalapur, C.S. Jha, "Estimation of above ground biomass in indian tropical forested area multifrequency DLR-ESAR data", *International Journal Of Geomatics and Geoscience*, Volume 1, No 2, ISSN 0976 – 4380, pg 167-178, 2010.
- [4] R. Bindlish, A. P. Barros, "Parameterization of vegetation backscatter in radar-based,soil moisture estimation", *Elsevier,Remote Sensing of Environment* vol. 76, PII: S0034-4257(00)00200-5 pp.130 – 137, 2001.
- [5] M. Santoro, L. Eriksson, J. Askne, C. Schmullius, "Assessment of stand-wise stem volume retrieval in boreal vegetation from JERS-1 L-band SAR backscatter", *International Journal of Remote Sensing*,Vol. 27, No. 16, 20, pp. 3425–3454,August 2006.
- [6] S.S. Saatchi, M. Moghaddam, "Estimation of crown and stem water content and biomass of boreal vegetation using polarimetric SAR imagery", *IEEE Transactions on Geoscience and Remote Sensing*, Vol. 38, No. 2,pp 697-709, March 2000.
- [7] T. M. Lillesand, R.W.Kiefer, J. W. Chipman, *Remote Sensing and Image Interpretation*, John Wiley & Sons(ASIA),PTE. LTD., Fifth Edition, pp. 638-732.
- [8] T.L. Ainsworth, J.P. Kelly, J.-S. Lee, "Classification comparisons between dual-pol, compact polarimetric and quad-pol SAR imagery", *ISPRS Journal of Photogrammetry and Remote Sensing* vol. 64, pp.464-471, 2009.
- [9] R. Dutta, "Assessment of tea bush health and yield using geospatial techniques", *ITC, International Institute for geo-information science and earth observation*, January 2006, pp. 1-70.
- [10] J. Dong, R. K. Kaufmann, R. B. Myneni, C. J. Tucker, P. E. Kauppi, J. Liski, W. Buermann, V. Alexeyev, M. K. Hughes, "Remote sensing estimates of boreal and temperate forest woody biomass: carbon pools sources and sinks", *Remote Sensing of Environment*, vol. 84,Issue 3, pg. 393–410, March 2003.
- [11] D.H.Hoekman, "Radar remote sensing data for application in forestry", *Agricultural University,Wageningen*,1990,pg 1-277.
- [12] S. Kumar, "Retreival of forest parameters from Envisat ASAR data for biomass inventory in dudhwa national park, U.P.,India", *ITC,International Institute for geo-information science and earth observation*, January 2009, pg. 1-85.

- [13] T. Svoray, M. Shoshany, “SAR based estimation of areal above ground biomass (AAB) of herbaceous vegetation in the semi-arid zone: A modification of the water cloud model”, *International Journal of Remote sensing*, Vol. 23, No. 19, pp 4089-4100, 2002.
- [14] L. E. B. Eriksson, J. Askne, M. Santoro, C. Schmullius , A. Wiesmann, “Stem volume retrieval with spaceborne L-band repeat-pass coherence : multi-temporal combination for boreal forest”, *IEEE Transactions on Geoscience and Remote Sensing*, pg. 3591-3594, 2005
- [15] Advanced Land Observing Satellite, Daichi, EORC, JAXA, research and application project, http://www.eorc.jaxa.jp/ALOS/en/about/about_index.htm, August,21,2011, 13:00hrs.
- [16] A. Freeman, S.L.Durdan, “A three component scattering model for polarimetric SAR data”, *IEEE Transactions on Geoscience and Remote Sensing*, vol. 36, NO. 3, pp. 963-973, May 1998.
- [17] D. Lu, “The potential and challenge of remote sensing-based biomass estimation”, *International Journal of Remote Sensing*, vol. 27, No. 7, pp.1297-1328, 10 April 2006.
- [18] A. K. Tiwari, J. S. Singh, “Analysis of forest land use and vegetation in a part of central Himalayas using aerial photographs”, *Environmental Conservation*, vol.14, pp. 233-244, 1987.
- [19] E. Tomppo, M. Nilsson, M. Rosengren, P. Aalto, P. Kennedy, “Simultaneous use of Landsat-TM and IRS-1C WiFS data in estimating large area tree stem volume and above ground biomass”, *Remote Sensing of Environment*, Vol. 82, pp.156-171, 2002
- [20] M. D. Behera, S. P. S. Kushwaha, P. S. Roy, “Forest vegetation characterization and mapping using IRS-1C satellite images in eastern Himalayan region”, *Geocarto International*, Vol. 16, No. 3, pp. September 2001.
- [21] B. Mohns, G.B. Applegate, D.A. Gilmour, “Biomass and productivity estimations for community foret management: A case study from the hills of Nepal-II. Dry matter productions in mixed young stands of chir pine (*Pinusroxburghii*) and broad-leaved species”, *Biomass*, Vol. 17, pp. 165-184, 1988.
- [22] M. H. Phua, H. Saito, “Estimation of biomass of a mountaneous tropical forest using landsat TM data”, *Canadian Journal of Remote Sensing*, Vol. 29, No. 4, pp. 429-440, 2003.
- [23] S. C. Popescu, R.H. Wynne, R.F. Nelson, “Measuring individual tree crown diameter with lidar and assessing its influence on estimating forest volume and biomass”, *Canadian Journal of Remote Sensing*, Vol. 29, No. 5, pp. 564-577, 2003.
- [24] T. Mette, K.P. Papathanassiou, I. Hajnsek, R. Zimmermann, “Forest biomass estimation using polarimetric SAR interferometry”, *IEEE Transactions on Geoscience and Remote Sensing*, vol. 36, No.3, pp. 817-819, 2002.
- [25] D. Zianis, P. Muukkonen, R. Makipaa, M. Mencuccini, “Biomass and stem volume equations for tree species in europe”, *Silva Fennica, The Finnish Society of Forest Science, The Finnish Forest Research Institute, Monographs* 4, pp. 1-63, Sep. 2005
- [26] D.N. Barua, *Science and Practice in Tea Culture*, Tea Research Association, India, Second Edition, March 2008, pp. 1-611.

- [27] G. S. Haripriya, “Estimates of biomass in Indian forests”, *Biomass and Bioenergy*, Vol. 19, pp.245-258, 2000.
- [28] E.P.W. Attema, F.T. Ulaby, “Vegetation modeled as a water cloud”, *Radio Science*, Vol. 13, No. 2, pp. 357-364, march-April 1978.
- [29] Y. Yamaguchi, A. Sato, W.M. Boerner, R. Sato, H. Yamada, “Four component scattering power decomposition with rotation of coherency matrix”, *IEEE Transactions on Geoscience and Remote Sensing*, vol. 49, NO. 6, pp. 2251-2258, June 2011.
- [30] S.R. Cloude, *Polarisation-applications in remote sensing*, Oxford University Press, First Edition 2010, pp. 1-453.
- [31] D.P. Lusch, *Introduction to microwave remote sensing*, BSRSI, Centre for remote sensing and GIS, Michigan State University, pp. 1-84, Nov. 1999.
- [32] J.C. Curlander, R.N. McDonough, *Synthetic Aperture Radar-Systems and signal processing*, John Wiley & Sons, Inc., 1991, pp. 1-647.
- [33] I. H. Woodhouse, *Introduction to microwave remote sensing*, Taylor & Francis, 2009, pp. 1-370.
- [34] help files associated with the POLSAR PRO software.
- [35] C.D. Richardson, “Polarimetric scattering model for multilayered vegetation in tropical forest”, *ITC, International Institute for geo-information science and earth observation*, April 2011.
- [36] Toklai Experimental Station(TRA), <http://www.tocklai.net/Cultivation/>, accessed on 19/01/2012 at 22:40 hrs.
- [37] J. Askne, P.B.G. Dammert, P. Fransson, H. Israelsson, L.M.H. Ulander, “Retreival of forest parameters using intensity and repeat pass interferometric SAR information : Proceedings of retrieval of Bio and Geophysical parameters from SAR data for land Application”, pp.119-129, 1995.
- [38] J. Askne, M. Santoro, G. Smith, E.S. Fransson, “Multitemporal repeat pass SAR interferometry of boreal forests, *IEEE Transactions on Geoscience and Remote Sensing*, vol. 41, No. 7, pp. 1540-1550, 2003.
- [39] Y.S. Zhou, W. Hong, F.Cao, “Investigations on volume scattering for vegetation parameter estimation of polarimetric SAR Interferometry”, *PIERS Online*, Vol. 5, No. 1, pp. 1-5, 2009.
- [40] Y. Yamaguchi, Y. Yajima, H. Yamada, “A four component decomposition of POLSAR images based on the coherency matrix”, *IEEE Transactions on Geoscience and Remote Sensing*, vol. 3, No. 3, pp. 292-296, July 2006.
- [41] S.R. Cloude, E. Pottier, “A review of target decomposition theorems in radar polarimetry”, *IEEE Transactions on Geoscience and Remote Sensing*, vol. 34, NO. 2, pp. 498-518, March 1996.

- [42] T. Mette, K.Papathanassiou, I. Hajnsek, "Biomass estimation from polarimetric SAR interferometry over heterogeneous forest terrain," *IEEE Transactions on Geoscience and Remote Sensing*, vol., NO., pp. 511-514, 2004.
- [43] Y. Yamaguchi, T. Moriyama, M. Ishido, H. Yamada, "Four component scattering model for polarimetric SAR image decomposition", *IEEE Transactions on Geoscience and Remote Sensing*, vol. 43, No. 8, pp. 1699-1706, August 2005.
- [44] O. Antropov, Y. Rauste, T. Häme, "Volume scattering modelling in PolSAR decompositions : study of ALOS PALSAR data over boreal forest", *IEEE Transactions on Geoscience and Remote Sensing*, vol. 49, No. 10, pp. 3838-3848, 2011.
- [45] A. Sato, Y. Yamaguchi, G. Singh, S.E. Park, "Four component scattering power decomposition with extended volume scattering model", *IEEE Geoscience and Remote Sensing Letters*, vol. 9, No. 2, pp. 166-170, March 2012.
- [46] D. P. Lusch, *Introduction to Microwave Remote Sensing*, Basic Science and Remote Sensing Initiative, Department of Geography, Michigan State University (BSRSI), Nov. 1999, pp. 1-84.
- [47] S.V. Nghiem, S.H. Yueh, R. Kwok, F.K. Li, "Symmetry properties in polarimetric remote sensing", *Radio Science*, vol. 27, No. 5, pp. 693-711, Sep-Oct.1992.
- [48] M. Molinier, J. Laaksonen, Y. Rauste, T. Hame, "Detecting changes in polarimetric SAR data with content based image retrieval", *Geoscience and remote sensing symposium, IGARSS, IEEE International*, pp. 2390-2393, 2007.
- [49] S. Quegan, T.L. Toan, H. Skriver, J. Gomez Dans, M.C. Gonzalez Sampedro, D.H. Hoekman, "crop classification with multitemporal polarimetric SAR data", *Workshop on POL-INSAR applications of SAR polarimetry and polarimetric interferometry* (ESA SP-529), Jan 2003.
- [50] M. Santoro, J. Askne, G. Smith, J.E.S. Fransson, "Stem volume retrieval in boreal forests from ERS1/2 interferometry", *Remote Sensing of Environment*, vol. 81, pp. 19-35, 2002.
- [51] A. N. Arslan, J. Koskinen, J. Pulliainen, M. Hallikainen, "A semi-empirical backscattering model of forest canopy covered by snow using SAR data", *IEEE Transactions on Geoscience and Remote Sensing*, vol. 5, pp. 1904-1906, 2000.
- [52] J. Askne, P. B. G. Dammert, P. Fransson, H. Israelsson, L.M.H. Ulander, "Retreival of forest parameters using intensity and repeat pass interferometric SAR information", *Proceedings of retrieval of Bio and Geophysical parameters from SAR data for land applications*, pp. 119-129, 1995.
- [53] J.T. Pulliainen, K. Heiska, J. Hyypä, M.T. Hallikainen, "Backscattering properties of boreal forests at the C and X bands", *IEEE Transactions on Geoscience and Remote Sensing*, vol. 32, No. 5, pp. 1041-1050, 1994.
- [54] efunda math forum, <http://www.efunda.com/math/leastsquares/leastsquares.cfm>, accessed on 19/02/2012 at 16:16 hrs.
- [55] J. J. Vanzyll, Y. Kim, M. Arii, "Requirements for model based polarimetric decomposition", *IEEE Geoscience and Remote Sensing Letters*, vol. 5, pp. V-417-V-420, 2008.

- [56] C.G.Brown, K.Sarabandi, “Estimation of red pine tree height using shuttle radar topography mission and ancillary data”, *IEEE Geoscience and Remote Sensing Letters*, vol. 4, pp. 2850-2852, 2003.
- [57] K.M. Viergever, I.H. Woodhouse, A. Marino, M. Brolly, N. Stuart, “backscatter and interferometry for estimating above ground biomass of sparse woodland: a case study in Belize”, *IEEE Geoscience and Remote Sensing Symposium, IGARSS*, vol. 3, pp. III-1047-III-1050, 2009.
- [58] J. Dong, R.K. Kaufmann, R.B. Myneni, C.J. Tucker, P.E. Kauppi, J. Liski, W. Beurmann, V. Alexeyev, M.K. Hughes, “Remote sensing estimatesof boreal and temperate forest woody biomass carbon pools sources and sinks”, *Remote Sensing of Environment*, vol. 84, Issue 3, pp. 393-410, March 2003.
- [59] J. O. Hagberg, L.M.H. Ulander, J. Askne, “Repeat pass SAR interferometry over forested terrain”, *IEEE Transactions on Geoscience and Remote Sensing*, vol. 33, issue 2, pp. 331-340, March 1995.
- [60] M.C. Dobson, F.T. Ulaby, T. LeToan, A. Beaudoin, E.S. Kasischke, N. Christensen, “Dependance of radar backscatter on coniferous forest biomass”, *IEEE Transactions on Geoscience and Remote Sensing*, vol. 30, issue 2, pp. 412-415, March 1992.
- [61] Y.A. Hussin, R.M. Reich, R.M. Hoffer, “Estimating splash pine biomass using radar backscatter”, *IEEE Transactions on Geoscience and Remote Sensing*, vol. 29, issue 3, pp. 427-431, May 1991.
- [62] H. Wang, K. Ouchi, “A simple moment method of forest biomass estimation from non-gaussian texture information by high-resolution polarimetric SAR”, *IEEE Transactions on Geoscience and Remote Sensing*, vol. 7, No. 4, pp. 811-815, October 2010.
- [63] N.S. Goel, “Models of vegetation canopy reflectance and their use in estimation of biophysical parameters from reflectance data”, *Remote Sensing Reviews*, vol. 4, pp. 1-212, 1988.
- [64] J.W. Trevett, *Imaging radar for resources surveys*, Chapman & Hall, London, GB, 1988, pp. 1-313.
- [65] P.S. Thenkabail, N. Stucky, B.W. Griscom, M.S. Ashton, J. Diels, B. van der Meer, E. Enclona, “Biomass estimation and carbon stock calculations in the oil palm plantations of African derived savannas using IKONOS data”, *International Journal of Remote Sensing*, vol. 25, issue 23, pp. 5447-5472, 2004.
- [66] M.A. Karam, A. K. Fung, R. H. Lang, and N. S. Chauhan, “A microwave scattering model for layered vegetation”, *IEEE Transactions on Geoscience and Remote Sensing*, vol. 30, No. 4, pp. 767-784, 1992.
- [67] F.T.Ulaby, K. McDonald, K. Sarabandi, M.C.Dobson, “Michigan microwave canopy scattering models (MIMICS)”, *Proceedings of IGARSS 88 symposium*, Winburg, Scotland.

- [69] D. S. Culvenor, "Extracting Individual Tree Information", *Remote Sensing of Forest Environments: Concepts and Case Studies*, M. A. Wulder and S. E. Franklin, eds., Kluwer Academic Press, 2003, pp. 255-277..
- [70] K. M. Viergever, I. H. Woodhouse and N. Stuart, "Airborne synthetic aperture radar for estimating above-ground biomass of the woody vegetation in tropical savannah woodland," *Proc. IGARSS 2006*, Denver, CO, vol. 1, pp. 3595-3598, 31 Jul.-4 Aug., 2006

9. APPENDIX A

9.1. LIST OF SYMBOLS

A	Amplitude of the radar signal
B	Above ground Biomass
$\sigma_{i,j}^{\circ}$	Sigma nought at image line and column i,j
θ	SAR incidence angle
η	Area fill factor
ψ	Two way attenuation
σ°	Backscatter cross section
σ_{tot}°	Total backscattered value
σ_{sur}°	Surface backscattered value
σ_{vol}°	Backscattered value due to volume scattering
λ	Wavelength
ρ	Specific gravity
π	Constant (3.1415)
V	volume
S_{VH}	Scattering matrix element
E	Scattered wave field
C	Covariance matrix
T	Coherency matrix
K	Target vector
γ	Scattered power
ϕ	Absolute phase

p,q	Components of scattering matrix
f_v	Model for volume scattering
f_s	Model for surface scattering
P	Total power
hrs	Hours
km	Kilometre
m	Metre(s)
t/ha.	Tons per hectare
r	Radius
h	Height of bush
G	Girth of stem
B_{tot}	Total biomass
I	Real component of the scattering elements
Q	Imaginary component of the scattering elements
f_c	Canopy scattering model
$M_{i,j}$	Composite scattering matrix with i,j as the constituent components
σ_{veg}°	Backscattered value due to scattering from vegetation (canopy)
dB	decibels

10. APPENDIX B

10.1. LIST OF SYMBOLS

AGB	Above Ground Biomass
SAR	Synthetic Aperture Radar
H,V	Horizontal, Vertical
WCM	Water Cloud Model
NDVI	Normalised Difference Vegetation Index
RADAR	RAdio Detection And Ranging
POLSAR	POLarimetric Synthetic Aperture Radar
PALSAR	Phased Array L-band Synthetic Aperture Radar
ALOS	Advanced Land Observing Satellite
RGB	Red-Green-Blue
SLC	Single Look Complex
RMSE	Root Mean Square Error